is regarded as a drug transporter which transports not only naturally occurring amino acids but also amino acid-related drugs such as L-dopa, a therapeutic drug for Parkinsonism; melphalan, an anti-cancer phenylalanine mustard; triiodothyronine and thyroxine, two thyroid hormones; gabapentin, an anti-convulsant and *S*-(1,2-dichlorovinyl)-L-cysteine, a neurotoxic cysteine conjugate [1,4–9].

By means of expression cloning, we isolated a LAT1 (L-type amino acid transporter 1), the first isoform of system L amino acid transporter, from C6 rat glioma cells [10]. It is a predicted 12-membrane-spanning protein [10]. It mediates Na^+-independent amino acid exchange and prefers large neutral amino acids with bulky or branched side chains for its substrates [10–12]. It requires an additional single-membrane-spanning protein the heavy chain of 4F2 antigen (4F2hc) for its functional expression in the plasma membrane [10,11,13–16]. LAT1 and 4F2hc form a heterodimeric complex via a disulfide bond [10,11,13–16]. The LAT1 mRNA is only expressed in restricted organs such as brain, spleen, placenta and testis [10,11,16,17]. However, the 4F2hc mRNA is ubiquitously expressed in all embryonic and adult tissues [10,11,16]. In addition, the LAT1 is highly expressed in malignant tumors presumably to support their continuous growth and proliferation [10,11,18,19].

Subsequently, we and other researchers cloned a LAT2 (L-type amino acid transporter 2), the second isoform of system L amino acid transporter [20–22]. The LAT2 is also a Na^+-independent amino acid transporter and requires the 4F2hc for its functional expression [20–22]. The LAT2 more ubiquitously expressed than LAT1 and transports not only large neutral amino acids but also small neutral amino acids in a fashion that appears to have broader substrate selectivity than LAT1 [20–23].

As mentioned above, it is proposed that the manipulation of system L activity in particular that of LAT1 would have therapeutic implications. The inhibition of LAT1 activity in tumor cells could be effective in the suppression of tumor cell growth by depriving of essential amino acids in tumor cells [9,24]. Up to now, the functional properties of LAT1 have been studied formerly by injecting LAT1 cRNA into *Xenopus* oocytes which is not well suited for investigating the characteristics of LAT1 such as using chemical compounds [10–12,14,16,17].

Oral cancer is the sixth most common cancer globally [25]. In the East and South Asian countries, the incidence is much higher where oral cancers constitute up to 25% of all malignancies [25]. However, the expression and functional characterization of amino acid transporters including the system L amino acid transporter for supplying nutrition to cells in the oral cancer cells are not known at all. In the present study, therefore, we examined the expressions of system L amino acid transporters and the properties of L-leucine transport in KB human oral epidermoid carcinoma cells. We report here that the majority of [^{14}C]L-leucine uptake in KB human oral epidermoid carcinoma cells is almost exclusively mediated by LAT1 with its associating protein 4F2hc. And we also propose that the KB cell system would be an excellent tool to investigate the characteristics of LAT1 and the specific inhibition of LAT1 in human oral squamous cell carcinomas will be a new rationale for anti-cancer therapy.

2. Material and methods

2.1. Materials

[^{14}C]L-Leucine was purchased from Perkin Elmer Life Sciences Inc. (Boston, MA). Affinity-purified rabbit anti-LAT1, anti-LAT2 and anti-4F2hc polyclonal antibodies were kindly provided by Kumamoto Immunochemical Laboratory, Transgenic Inc. (Kumamoto, Japan). Anti-rabbit-horseradish peroxidase conjugated-secondary antibody and envision (+) rabbit peroxidase were purchased from Jackson ImmunoResearch Laboratories Inc. (West Grove, PA) and DAKO (Glostrup, Denmark), respectively. Other chemicals were purchased from Sigma (St Louis, MO). KB human oral epidermoid carcinoma cells were provided by American Type Culture Collection (ATCC, Rockville, MD).

2.2. Cell culture

KB cells were grown in DMEM and F-12 media with the ratio of 3:1 supplemented with 10% FBS [26]. Cells were maintained as monolayers in plastic

culture plate at 37 °C in a humidified atmosphere containing 5% CO_2.

2.3. RT-PCR analysis

RNA was prepared from KB cells maintained in the growth medium at 37 °C by RNA preparation kit (Isogen, Nippon-Gene, Japan) in accordance with the manufacturer's instruction. Poly(A)$^+$RNA was selected by oligo(dT) cellulose chromatography (Amersham Pharmacia Biotech) [27].

For RT-PCR analysis, the first-strand cDNAs were prepared from KB cell poly(A)$^+$RNA using SuperScript First-Strand Synthesis System for RT-PCR (Life Technologies Inc.) with an oligo dT primer, and used as a template for PCR amplification. The PCR amplification was performed using Taq polymerase Amplitaq Gold (Roche Molecular Systems Inc.) in the following protocol: 94 °C for 12 min, followed by 25 cycles of 94 °C for 30 s, 60 °C for 30 s and 72 °C for 40 s and a final extension step of 72 °C for 30 min [28,29]. A pair of primers, 5′-TTCATCGCAGTACATCGTGG-3′ (491–510 bp) and 5′-CCCAGGTGATAGTTCCCGAA-3′ (1008–1027 bp), was used for PCR amplification of LAT1. A pair of primers, 5′-AGCCCTGAAGAAAGAGATCG-3′ (811–830 bp) and 5′-TGCATATCTGTACAATCCCC-3′ (1321–1340 bp), was used for PCR amplification of LAT2. A pair of primers, 5′-TCGATTACCTGAGCTCTCTG-3′ (551–570 bp) and 5′-GGGATTTTGTATGCTCCCCA-3′ (1041–1060 bp), was used for PCR amplification of 4F2hc.

2.4. Real-time quantitative RT-PCR

For real-time quantitative RT-PCR analysis, total RNA was prepared from KB cells using an RNA preparation kit (Isogen, Nippon-Gene, Japan) following the manufacturer's instructions. The total RNA was treated with DNase I (Boehringer Mannheim; 1 unit per 10 mg of RNA) at 25 °C for 20 min. First strand cDNA was produced using SuperScript First-Strand Synthesis System for RT-PCR (Life Technologies Inc.) with an oligo dT primer [30]. Five-microgram of total RNA was used for a reverse transcription reaction (20 μl). For the real-time quantitative PCR, 1 μl out of the 20 μl reverse transcription reaction mixture was used.

Standard first strand cDNAs for LAT1, LAT2 and 4F2hc were synthesized from each cRNA. LAT1 cRNA was obtained by in vitro transcription using T3 RNA polymerase from the LAT1 cDNA (GenBank/EMBL/DDBJ accession no. AB018009) in pBluescript II SK$^-$ (Stratagene) linearized with *Xho*I [31]. LAT2 and 4F2hc cRNAs were also obtained by in vitro transcription using SP6 RNA polymerase for LAT2 cDNA (GenBank/EMBL/DDBJ accession no. AB037669) in pSPORT 1 (Life Technologies Inc.) linearized with RsrII and T7 RNA polymerase for 4F2hc cDNA (GenBank/EMBL/DDBJ accession no. AB018010) in pBluescript II SK$^-$ linearized with *Bam*HI, respectively [31]. The first strand cDNAs were synthesized as described above using cRNAs for LAT1, LAT2 and 4F2hc as templates [30].

The 7700 Sequence Detector System (Perkin Elmer/Applied Biosystems Inc.) was used for real-time quantitative RT-PCR analyses [32]. The RT-PCR reaction mixture (50 μl) included reverse transcription products corresponding to 250 ng of total RNA or standard first strand cDNAs corresponding to 25 fg–25 ng of cRNA, 25 μl of Taqman Universal PCR Master Mix (Perkin Elmer/Applied Biosystems Inc.), 0.5 μl of forward and reverse primer (10 μM) and 1 μl of corresponding Taqman probe (5 μM) [32]. RT-PCR cycle parameters were 50 °C for 2 min, 95 °C for 10 min, followed by 40 cycles at 95 °C for 15 s and 60 °C for 1 min. The primers and the probes were designed using Primer Express software (Perkin Elmer/Applied Biosystems Inc.) and synthesized by Perkin Elmer/Applied Biosystems Inc. For LAT1, the forward and reverse primers were 5′-GATCCTGCTGGGCTTCGT-3′ and 5′-AGTTTGGTGCCTTCAAATGAGAA-3′, respectively, and the Taqman probe was 6FAM-AGATCGGGAAGGGTGATGTGTCCAATC-TAMRA [24]. For LAT2, the forward and reverse primers were 5′-AATGCATTTGAGAATTTCCAGGA-3′ and 5′-GAGCCCTGAAGGAAAGCCA-3′, respectively, and the Taqman probe was 6FAM-CCTGACATCGGCCTCGTCGCA-TAMRA [24]. For 4F2hc, the forward and reverse primers were 5′-CTCAGGCAAGGCTCCTGACT-3′ and 5′-GGCAGGGTGAAGAGCATCA-3′, respectively, and the Taqman probe was 6FAM-TGCCGGCTCAACTTCTTCGACTCTAC-TAMRA [24]. The concentration of reverse and

forward primers used was 900 nM for each. The concentration of probe was 250 nM.

2.5. Western blot analysis

Protein samples from KB cells were prepared as described elsewhere [11,33–36], with minor modifications. Briefly, KB cells were washed with PBS and prepared by centrifugation 5 min at 1000 × *g*. The KB cells were homogenized in nine volumes of 50 mM Tris–HCl, pH 7.5, 25 mM KCl, 1 mM $MgCl_2$, 1 mM phenylmethylsulfonyl fluoride and 0.25 M sucrose, with 15 strokes of Dounce homogenizer. The homogenate was centrifuged for 10 min at 8000 × *g*, and the supernatant was centrifuged further for 1 h at 100,000 × *g*. After centrifugation, the membrane pellet was resuspended in 0.25 M sucrose, 100 mM KCl, 5 mM $MgCl_2$ and 50 mM Tris, pH 7.4. The protein samples were heated at 100 °C for 5 min in the sample buffer either in the presence (reducing condition) or absence (non-reducing condition) of 5% 2-mercaptoethanol and then subjected to SDS-polyacrylamide gel electrophoresis. The separated proteins were transferred electrophoretically to a Hybond-P polyvinylidene difluoride transfer membrane (Amersham Pharmacia Biotech). The membrane was treated with non-fat dried milk and diluted anti-LAT1 (1:1000 dilution), LAT2 (1:500 dilution) and 4F2hc (1:1000 dilution) affinity-purified antibodies [11,24,37] and then with horseradish peroxidase-conjugated anti-rabbit IgG as a secondary antibody (Jackson ImmunoResearch). The signals were detected with an ECL plus system (Amersham Pharmacia Biotech) [34–36].

2.6. Immunohistochemistry of KB cells

KB cells were plated at the density of 3×10^5 cells/well into 2-well chamber slides (Nalge Nunc International Corp.). After an overnight growth, KB cells were washed with PBS and fixed in 50% solution of methanol–acetic acid (3:1, v/v) for 5 min. The KB cells were rehydrated and incubated with affinity purified anti-LAT1 (1:100 dilution), anti-LAT2 (1:50 dilution) and anti-4F2hc (1:100 dilution) polyclonal antibodies at 4 °C overnight [11,24,37].

Thereafter, they were treated with envision (+) rabbit peroxidase (DAKO) for 30 min at room temperature. To detect immunoreactivity, the KB cells were treated with diaminobenzidine (0.8 mM) [34,36]. For absorption experiments, the KB cells were treated with the primary antibodies in the presence of antigen peptides (200 μg/ml) [38]. The KB cells were counterstained with hematoxylin.

2.7. Uptake measurements in KB cells

KB cells were maintained in the growth medium at 37 °C in 5% CO_2. The cells were collected and seeded on 24-well plates (1×10^5 cells/well) in the fresh growth medium. The uptake measurements were performed at 48 h after seeding.

After the removal of the growth medium, the cells were washed 3 times with the standard uptake solution (125 mM NaCl, 4.8 mM KCl, 1.3 mM $CaCl_2$, 1.2 mM $MgSO_4$, 25 mM HEPES, 1.2 mM KH_2PO_4, 5.6 mM Glucose, pH 7.4) or Na^+-free uptake solution (125 mM choline-Cl, 4.8 mM KCl, 1.3 mM $CaCl_2$, 1.2 mM $MgSO_4$, 25 mM HEPES, 1.2 mM KH_2PO_4, 5.6 mM Glucose, pH 7.4), and preincubated for 10 min at 37 °C. Then, the medium was replaced by the uptake solution containing [^{14}C]L-leucine. The uptake was terminated by removing the uptake solution followed by washing 3 times with ice-cold uptake solution [34,39]. Then, cells were solubilized with 0.1 N NaOH and radioactivity was counted by liquid scintillation spectrometry. The values are expressed as pmol/mg protein/min. For the measurement of the uptake of [^{14}C]L-leucine, four to six wells of KB cells were used for each data point. To confirm the reproducibility of the results, three separate experiments were performed for each measurement. Results from the representative experiments are shown in figures.

For the inhibition experiments, the uptake of 20 μM [^{14}C]L-leucine was measured in the presence or absence of 2 mM non-labeled test compounds, unless otherwise indicated [10–12].

K_m and V_{max} values were determined using Eadie–Hofstee plots based on the [^{14}C]L-leucine uptake measured for 1 min at 1, 10, 30, 100, 300 and 1000 μM.

2.8. Efflux measurements in KB cells

The KB cells were incubated for 10 min in the Na^+-free uptake solution containing 1 μM [^{14}C]L-leucine

Fig. 1. Detection of LAT1, LAT2 and 4F2hc by RT-PCR in KB cells. The first strand cDNA prepared from KB cell poly(A)$^+$RNA was used as template for PCR amplification. The PCR products were electrophoresed on a 1.2% agarose gel and visualized with ethidium bromide. The LAT1-specific PCR product (539 bp) and 4F2hc-specific PCR product (510 bp) were obtained from KB cells.

(2 μCi/ml) to load the KB cells with [^{14}C]L-leucine [10–12,24]. The KB cells were then washed 3 times with 37 °C Na^+-free uptake solution and incubated in 500 μl uptake solution with or without addition of test amino acids. After incubation, the incubation medium was removed from the well. Then, cells were solubilized with 0.1 N NaOH and the radioactivity was counted by liquid scintillation spectrometry. The radioactivity in the medium and the remaining radioactivity in the KB cells were measured. The values were expressed as % radioactivity (radioactivity of medium or KB cells/(radioactivity of medium + radioactivity of KB cells) [10,12,24].

The K_m values of the [^{14}C]L-leucine efflux induced by extracellularly applied L-leucine was determined using the Eadie–Hofstee plot based on the [^{14}C]L-leucine efflux measured for 1 min at 10, 30, 100, 300 and 1000 μM of extracellularly applied L-leucine [12,24].

2.9. Data analysis

All experiments were performed in triplicate. Results are presented as mean ± SEM. Statistical significance was analyzed by using Student's *t*-test for two groups and one way analysis of variance for multi-group comparisons. $P < 0.05$ is considered statistically significant.

3. Results

3.1. Detection of LAT1 and 4F2hc in KB cells

In RT-PCR analysis, the PCR products for LAT1 and its associating protein 4F2hc were detected in KB cells, whereas the LAT2 was not detected in KB cells (Fig. 1).

The presence of LAT1 and 4F2hc in KB cells was further examined by real-time quantitative RT-PCR. In the real-time quantitative RT-PCR, LAT1 and 4F2hc was detected in KB cells (data not shown). The amount of LAT1 and 4F2hc was very similar in KB cells ($32.85 \pm 1.97 \times 10^{-18}$ mol/1 g total RNA versus $28.49 \pm 1.45 \times 10^{-18}$ mol/1 g total RNA). Consistent with the result form the RT-PCR analysis (Fig. 1), LAT2 was not detected in KB cells in real-time quantitative RT-PCR (data not shown).

Western blot analysis was performed on the membrane fractions prepared from KB cells. The antibodies raised against LAT1 (Fig. 2A) and 4F2hc (Fig. 2C) both recognized the 125 kDa protein band under the non-reducing condition, whereas this band

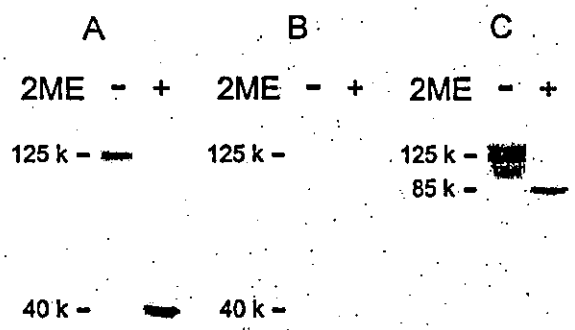

Fig. 2. Association between of LAT1 and 4F2hc proteins in KB cells. Western blot analysis was performed on the membrane fraction prepared from KB cells in the presence or absence of 2-mercaptoethanol using an anti-LAT1 antibody, an anti-LAT2 antibody and an anti-4F2hc antibody. For LAT1 (A) the 125 kDa protein band detected in the absence of 2-mercaptoethanol ('2ME − ') was not detected in the presence of 2-mercaptoethanol ('2ME + '), and a 40 kDa protein band was detected instead. For 4F2hc (C) the 125 kDa protein band detected in the absence of 2-mercaptoethanol (2ME −) shifted to an 85 kDa protein band by the treatment of 2-mercaptoethanol (2ME +). For LAT2 (B) any protein band did not detect both in the absence (2ME −) and presence of 2-mercaptoethanol (2ME +).

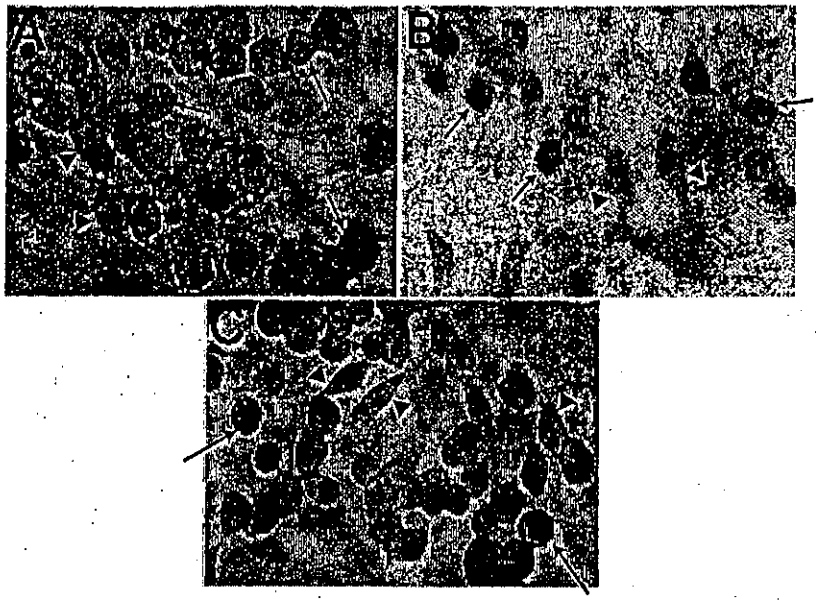

Fig. 3. Immunodetection of LAT1, LAT2 and 4F2hc in KB cells. Immunohistochemistry was performed on KB cells as described in Section 2. LAT1 immunoreactivity (A) was detected on the plasma membrane and 4F2hc immunoreactivity (C) was detected on the plasma membrane and cytoplasm in KB cells, indicating the coexistence of LAT1 and 4F2hc in the plasma membrane of KB cells. LAT2 immunoreactivity (B) was not detected not only on the plasma membrane but also cytoplasm in KB cells. Arrowheads indicate sharp type cells. Arrows indicate round type cells.

shifted to the 40 kDa protein band for LAT1 (Fig. 2A) and 85 kDa protein band for 4F2hc (Fig. 2C) under the reducing condition. The protein band for LAT2 was not detected for the membrane fractions prepared from KB cells both under the reducing and non-reducing conditions (Fig. 2B).

In the immunohistochemical analysis, LAT1 and 4F2hc proteins were detected in KB cells (Fig. 3A and C), but LAT2 proteins were not detect in KB cells (Fig. 3B). LAT1 and 4F2hc were found to be mainly colocalized in the plasma membrane. In the absorption experiments in which the KB cell plates were treated with the primary antibodies in the presences of LAT1, LAT2 and 4F2hc antigen peptides (200 μg/ml), the immunoreactivities were not detected, confirming the specificities of the immunoreactions (data not shown). The results from RT-PCR, real-time quantitative RT-PCR, Western blot and immunohistochemical analyses indicate that LAT1 but not LAT2 is present together with 4F2hc in the plasma membrane of KB human oral epidermoid carcinoma cells.

3.2. The properties of [^{14}C]L-leucine uptake by KB cells

The properties of [^{14}C]L-leucine transport were examined in KB cells. As shown in Fig. 4A, the level of [^{14}C]L-leucine uptake (20 μM) by KB cells measured in the standard uptake solution was not altered by replacing NaCl of the uptake solution with choline-Cl, indicating that L-leucine uptake by KB cells is Na^+-independent. In the subsequent experiments, the transport measurements were performed under Na^+-free conditions. When the uptake measurements were performed on ice, the [^{14}C]L-leucine uptake was not detected, confirming that the [^{14}C]L-leucine uptake by KB cells was due to the transporter-mediated transport (Fig. 4A). As shown in Fig. 4B, the uptake of [^{14}C]L-leucine (20 μM) was completely inhibited by 2 mM 2-aminobicyclo-(2,2,1)-heptane-2-carboxylic acid (BCH), a specific inhibitor of system L, indicating that system L is responsible for the [^{14}C]L-leucine uptake by KB cells.

To determine the time course of [^{14}C]L-leucine uptake by KB cells, the level of uptake was measured

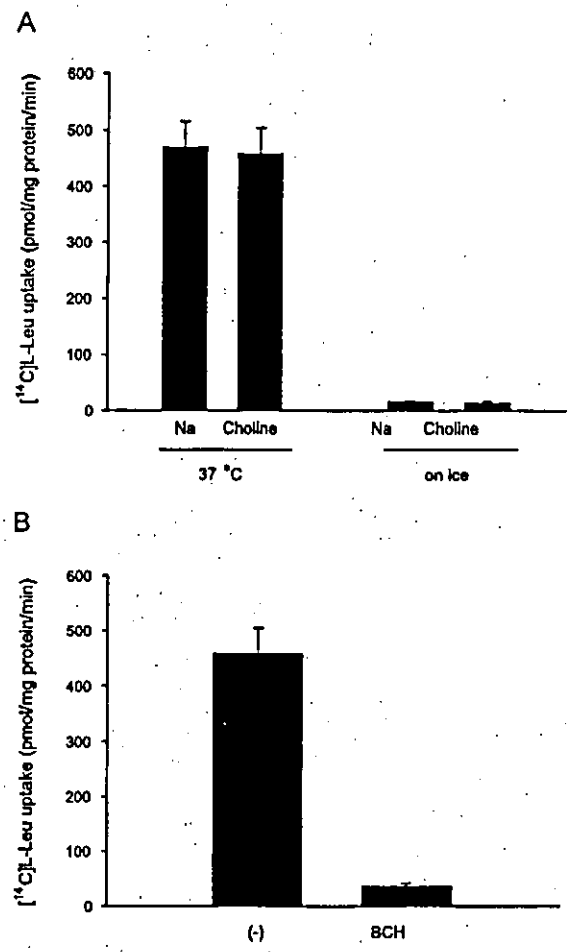

Fig. 4. The [^{14}C]L-leucine uptake by KB cells. (A) Ion dependence of [^{14}C]L-leucine transport. The [^{14}C]L-leucine (20 μM) uptake measured in the standard uptake solution (Na) was compared with that measured in the Na^+-free uptake solution (Choline). The [^{14}C]L-leucine transport measurement was performed at 37 °C and on ice. (B) Inhibition of [^{14}C]L-leucine transport by 2-aminobicyclo-(2,2,1)-heptane-2-carboxylic acid (BCH), a specific inhibitor of system L. The [^{14}C]L-leucine (20 μM) uptake was measured in the presence (BCH) or absence (−) of 2 mM BCH.

for 0.5–20 min. Uptake of [^{14}C]L-leucine (20 μM) was time-dependent and exhibited a linear dependence on the incubation time up to 1 min (Fig. 5A). So, subsequent uptake measurements were performed for 1 min and the values are expressed as pmol/mg protein/min. As shown in Fig. 5B, [^{14}C]L-leucine uptake was saturable and followed Michaelis–Menten kinetics with a K_m values of 65.9 ± 7.1 μM (mean ± SEM of three separate experiments) for [^{14}C]L-leucine uptake.

3.3. Inhibition of [^{14}C]L-leucine uptake by L-amino acids in KB cells

In order to examine which L-amino acids interact with L-leucine uptake mechanism in KB cells,

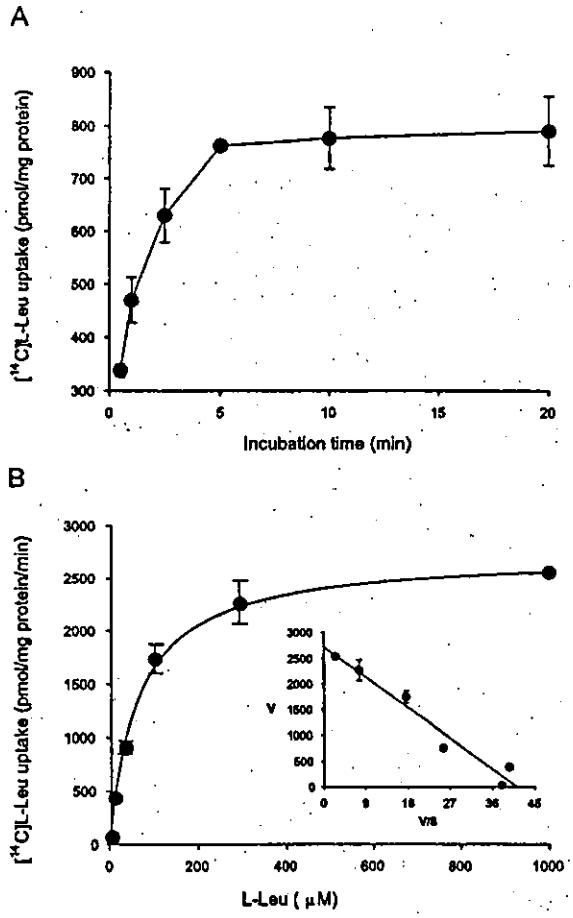

Fig. 5. Time course and concentration dependence of [^{14}C]L-leucine uptake by KB cells. (A) The dependence of [^{14}C]L-leucine uptake on the incubation time. The KB cells were incubated in the Na^+-free uptake solution containing 20 μM [^{14}C]L-leucine for 0.5, 1, 2.5, 5, 10 and 20 min. (B) Concentration dependence of [^{14}C]L-leucine transport in KB cells. The uptake of [^{14}C]L-leucine by KB cells was measured for 1 min and plotted against L-leucine concentration. The L-leucine uptake was saturable and fit to the Michaelis–Menten curve (K_m = 65.9 μM; V_{max} = 2725.8 pmol/mg protein/min). The inset shows an Eadie–Hofstee plot of L-leucine uptake that was used to determine the kinetic parameters.

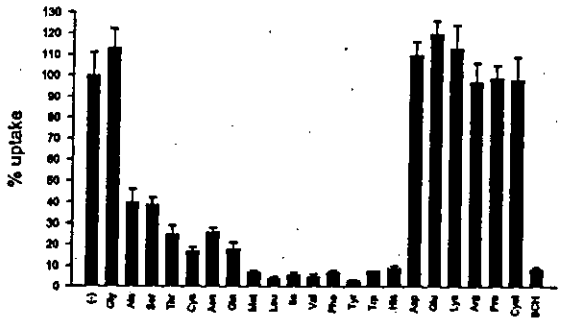

Fig. 6. Inhibition of [^{14}C]L-leucine uptake by L-amino acids in KB cells. The [^{14}C]L-leucine (20 μM) uptake was measured in the presence of 2 mM non-radiolabeled L-amino acids and system L specific inhibitor BCH in the Na^+-free uptake solution.

the [^{14}C]L-leucine uptake (20 μM) was measured in the presence of 2 mM non-labeled amino acids in the Na^+-free uptake solution. The [^{14}C]L-leucine uptake was highly inhibited by L-isomers of threonine, cysteine, asparagine, glutamine, methionine, isoleucine, valine, phenylalanine, tyrosine, tryptophan, histidine and BCH (Fig. 6). Alanine and serine exhibited weaker inhibitory effects on [^{14}C]L-leucine transport (Fig. 6). Glycine, aspartate, glutamate, lysine, arginine, proline and cystine have not revealed any inhibitory effects on [^{14}C]L-leucine transport in KB cells (Fig. 6).

3.4. The properties of [^{14}C]L-leucine efflux from KB cells

To examine the properties of [^{14}C]L-leucine efflux from KB cells, KB cells were loaded with [^{14}C]L-leucine by being incubated for 10 min in the Na^+-free uptake solution containing 1 μM [^{14}C]L-leucine. The efflux of loaded radioactivity was measured in the presence or absence of non-labeled L-leucine in the extracellular medium. The loaded [^{14}C]L-leucine detected about 50 or 60% in the extracellular medium within 1 min in the presence of extracellular 0.1 or 1 mM L-leucine, respectively (Fig. 7A). The extracellularly applied L-leucine induced the efflux of preloaded [^{14}C]L-leucine in a concentration-dependent manner (Fig. 7B). The K_m value of extracellularly applied L-leucine to induce the preloaded [^{14}C]L-leucine efflux was 60.6 ± 9.0 μM (mean ± SEM of three separate experiments).

3.5. [^{14}C]L-leucine efflux induced by L-amino acids

The amino acids that inhibited [^{14}C]L-leucine uptake in KB cells were investigated to examine

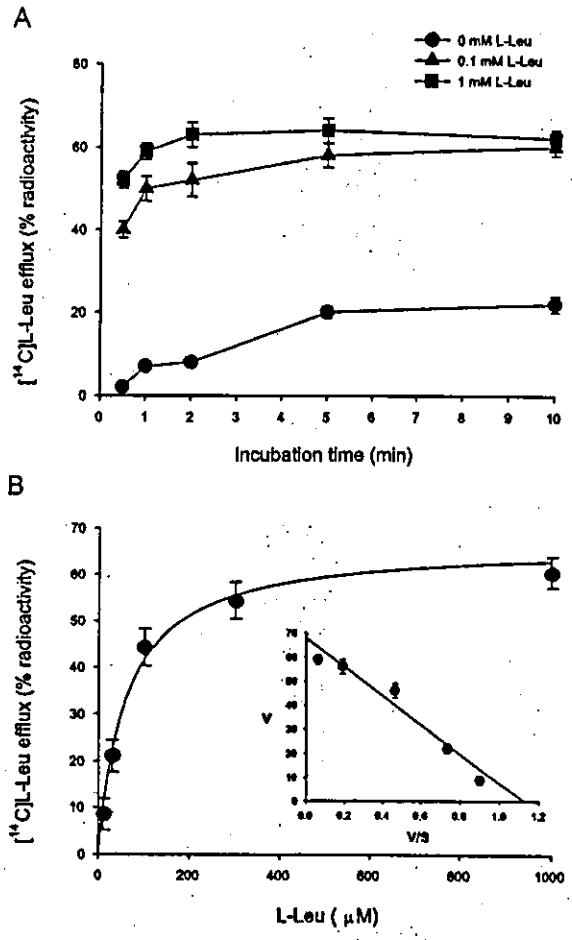

Fig. 7. The [^{14}C]L-leucine efflux from KB cells. (A) Time-course of [^{14}C]L-leucine efflux from KB cells preloaded with [^{14}C]L-leucine. The efflux was measured in the presence (0.1 mM L-Leu or 1 mM L-Leu) or absence (0 mM L-Leu) of L-leucine in the extracellular medium. The values are expressed as a percentage of the total radioactivity loaded to the KB cells (see Section 2). (B) The dependence of [^{14}C]L-leucine efflux on the concentration of extracellular L-leucine. The KB cells were preloaded with [^{14}C]L-leucine by being incubated in the Na^+-free uptake solution containing 1 μM [^{14}C]L-leucine for 10 min. The efflux of loaded [^{14}C]L-leucine induced by extracellularly applied L-leucine was measured for 1 min and plotted against extracellular L-leucine concentration. Inset: Eadie–Hofstee plot of the [^{14}C]L-leucine efflux used to determine kinetic parameters. The L-leucine efflux was saturable and fit to a Michaelis–Menten curve. The K_m and V_{max} values were 60.6 μM and 66.7% radioactivity, respectively.

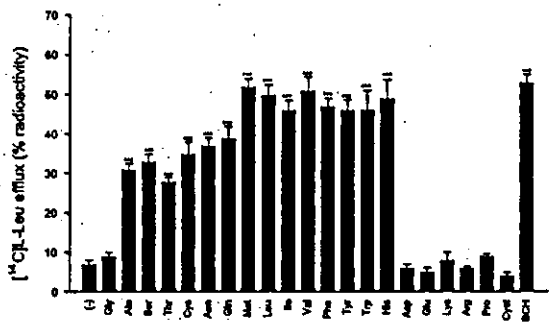

Fig. 8. Efflux of preloaded [^{14}C]L-leucine by L-amino acids from KB cells. The efflux of preloaded [^{14}C]L-leucine from the KB cells was measured for 1 min in the presence of 100 μM L-amino acids and BCH in the medium and compared with that measured in the absence of these amino acids (−). ***$P < 0.001$ versus control (the efflux measured in the absence of L-amino acids (−)).

whether they induce efflux of preloaded [^{14}C]L-leucine when applied extracellularly. As shown in Fig. 8, extracellularly applied L-methionine, L-leucine, L-isoleucine, L-valine, L-phenylalanine, L-tyrosine, L-tryptophan, L-histidine and BCH induced high level of efflux of preloaded [^{14}C]L-leucine. L-Alanine, L-serine, L-threonine, L-cysteine, L-asparagine and L-glutamine induced relatively low but significant efflux of the preloaded [^{14}C]L-leucine (Fig. 8). L-Glycine, L-aspartate, L-glutamate, L-lysine, L-arginine, L-proline and L-cystine did not induce the significant efflux of preloaded [^{14}C]L-leucine at all (Fig. 8).

4. Discussion

It has been known that the oral cancer is the sixth most common cancer globally [25]. Despite the introduction of novel therapeutic modalities into the treatment of oral cancer, improvements in long-term survival rates have only been modest. Advances in underlying mechanisms of oral cancer likely will be necessary to improve survival rates, which, despite better early detection of oral cancer, have plateaued over the past two decades and remain among the worst of all cancer site [40]. The system L amino acid transporters play an important role in the proliferation and continuous growth of cancer cells [10,11,18,19]. However, the expression and functional properties of amino acid transporters including the system L amino acid transporter for supplying organic nutrition to cells in the oral cancer cells have not been clarified entirely. In the present study, therefore, we investigated the expressions of system L amino acid transporters and the properties of L-leucine transport in KB human oral epidermoid carcinoma cells. By RT-PCR analysis (Fig. 1) and real-time quantitative RT-PCR analysis, we showed that KB cells express LAT1, an isoform of system L amino acid transporter, together with its associating protein 4F2hc, but do not express the other system L isoform LAT2. Consistent with our previous study that we performed on T24 human bladder carcinoma cells [11,24], we detected proteins for LAT1 and 4F2hc connected with each other via a disulfide bond on the membrane fraction prepared from KB cells in the Western blot analysis, but not detected protein for LAT2 (Fig. 2). We also performed the immunohistochemical analysis on KB cells and showed that LAT1 protein is present in the plasma membrane of KB cells with 4F2hc protein (Fig. 3). As these results correspond to our previous study that T24 human bladder carcinoma cells express LAT1 and 4F2hc but not LAT2 in the plasma membrane [24], it is concluded that KB human oral epidermoid carcinoma cells express system L amino acid transporter LAT1 but not LAT2 in the plasma membrane with 4F2hc.

In our previous study [24], the [^{14}C]L-leucine uptake measured in T24 cells was Na^+-independent and completely inhibited by the system L selective inhibitor BCH [1,24,41]. Although BCH is a selective inhibitor of system L [1,24,41], BCH also inhibits the transports of amino acids mediated by a Na^+-dependent neutral and basic amino acid transporter $ATB^{0,+}$ [42]. In the Na^+-free condition, however, it is still correct that BCH selectively inhibits the transports of amino acids mediated by system L amino acid transporters. In the present study, the [^{14}C]L-leucine uptake measured in KB cells was Na^+-independent and completely inhibited by BCH (Fig. 4). And the KB cells express only LAT1, one of the two system L transporters, in the plasma membrane. These results suggest that amino acid transporter LAT1 but not LAT2 plays an important role in the L-leucine uptake in KB human oral epidermoid carcinoma cells.

The [^{14}C]L-leucine uptake by KB cells is saturable and followed Michaelis–Menten kinetics (Fig. 5). The K_m value for the [^{14}C]L-leucine uptake was about

65 μM. This K_m value is relatively higher than those of human LAT1 [11] and rat LAT1 [10,12] expressed in *Xenopus* oocytes (~20 μM) and relatively lower than the K_m value for the [^{14}C]L-leucine uptake in T24 cells (~100 μM) [24]. This small difference may be due to different cell systems and conditions used [10–12,24].

The profiles of inhibition of [^{14}C]L-leucine uptake by L-amino acids in KB cells were basically identical to those determined for human LAT1 [11] and rat LAT1 [10,12] expressed in *Xenopus* oocytes and those performed for the profiles of inhibition of [^{14}C]L-leucine uptake by L-amino acids in T24 cells [24], except that [^{14}C]L-leucine uptake was more strongly inhibited by L-alanine, L-serine, L-threonine, L-cysteine, L-asparagine and L-glutamine in KB cells (Fig. 6). As already mentioned, the LAT1 is the predominant system L amino acid transporter in KB cells. Taken together, it is concluded that the majority of [^{14}C]L-leucine uptake is mediated by LAT1 with its associating protein 4F2hc, but not LAT2 in KB cells. These results also indicate that the KB cell system is an excellent tool to investigate for transport properties of various compounds via LAT1.

It has been known that LAT1 is an amino acid exchanger [10–12,24]. In the previous paper [12,24], we showed that the transportable substrates but not non-transportable blockers induced the effluxes of preloaded and radiolabeled substrates mediated by LAT1. In the present study, we performed efflux measurements in KB cells. The preloaded radioactivity was effluxed about 50% from KB cells to the medium within 1 min by responding to the extracellularly applied 100 μM L-leucine (Fig. 7A). The efflux of radioactivity was dependent on the concentration of the extracellularly applied L-leucine (Fig. 7B). The K_m value of extracellularly applied L-leucine to induce the preloaded [^{14}C]L-leucine efflux was about 60 μM. It is very similar to that of L-leucine uptake by KB cells (about 65 μM). We also examined whether the amino acids induce the efflux of preloaded [^{14}C]L-leucine by performing the efflux measurements in KB cells. Extracellularly applied L-alanine, L-serine, L-threonine, L-cysteine, L-asparagine, L-glutamine, L-methionine, L-leucine, L-isoleucine, L-valine, L-phenylalanine, L-tyrosine, L-tryptophan and L-histidine induced efflux of preloaded [^{14}C]L-leucine (Fig. 8). Moreover, BCH also induces high level of efflux of preloaded [^{14}C]L-leucine (Fig. 8). These substrates which enable to induce the efflux of preloaded [^{14}C]L-leucine were just same as the compounds which inhibited [^{14}C]L-leucine uptake in KB cells. Therefore, these amino acids and BCH are supposed to be transported by LAT1 in KB cells. These results from the efflux experiments in KB cells are in accordance with the concept of obligatory exchange for the transport mediated by LAT1 [10–12]. So, we suggested that the efflux measurement procedure can also be applicable to KB human oral epidermoid carcinoma cells. In addition, the KB cell system is also useful to develop drugs with efficient permeation utilizing LAT1 as a permeation path.

In the present study, we have characterized the [^{14}C]L-leucine uptake by KB cells and have suggested that the uptake is mediated by LAT1, an isoform of system L amino acid transporters. We also propose that the KB cell system is an excellent tool to investigate the characteristics of LAT1. The LAT1 is upregulated in tumor cells to support their continuous growth and proliferation and the LAT1 transports large neutral amino acids including several essential amino acids [1,18,19]. The LAT1 is, therefore, a major route through which KB human oral epidermoid carcinoma cells take up large neutral amino acids including several essential amino acids to support their continuous growth and proliferation and the inhibition of LAT1 would be a new rationale to suppress the growth of tumor cells including oral cancer cells.

Overall, the results of the present study demonstrate that the majority of [^{14}C]L-leucine uptake in KB human oral epidermoid carcinoma cells is mediated by LAT1 with its associating protein 4F2hc. Conclusively, these facts propose that the KB human oral epidermoid carcinoma cell is an excellent cell system to investigate the characteristics of LAT1 and the LAT1 would be a new target to inhibit the oral cancer cell growth.

Acknowledgements

This work was supported by grant No. (R01-2002-000-00165-0 (2002)) from the Basic Research Program of the Korea Science and Engineering

Foundation. Anti-LAT1, anti-LAT2 and anti-4F2hc polyclonal antibodies were supplied by Kumamoto Immunochemical Laboratory, Transgenic., Kumamoto, Japan.

References

[1] H.N. Christensen, Role of amino acid transport and countertransport in nutrition and metabolism, Physiol. Rev. 70 (1990) 43–77.
[2] J.D. McGivan, M. Pastor-Anglada, Regulatory and molecular aspects of mammalian amino acid transport, Biochem. J. 299 (1994) 321–334.
[3] D.L. Oxender, H.N. Christensen, Evidence for two types of mediation of neutral amino acid transport in Ehrlich cells, Nature 197 (1963) 765–767.
[4] G.J. Goldenberg, H.Y. Lam, A. Begleiter, Active carrier-mediated transport of melphalan by two separate amino acid transport systems in LPC-1 plasmacytoma cells in vitro, J. Biol. Chem. 254 (1979) 1057–1064.
[5] M. Lakshmanan, E. Goncalves, G. Lessly, D. Foti, J. Robbins, The transport of thyroxine into mouse neuroblastoma cells, NB41A3: the effect of L-system amino acids, Endocrinology 126 (1990) 3245–3250.
[6] J.P. Blondeau, A. Beslin, F. Chantoux, J. Francon, Triiodothyronine is a high-affinity inhibitor of amino acid transport system L1 in cultured astrocytes, J. Neurochem. 60 (1993) 1407–1413.
[7] T.Z. Su, E. Lunney, G. Campbell, D.L. Oxender, Transport of gabapentin, a gamma-amino acid drug, by system l alpha-amino acid transporters: a comparative study in astrocytes, synaptosomes and CHO cells, J. Neurochem. 64 (1995) 2125–2131.
[8] P. Gomes, P. Soares-da-Silva, L-DOPA transport properties in an immortalized cell line of rat capillary cerebral endothelial cells, RBE 4, Brain Res. 829 (1999) 143–150.
[9] Y. Kanai, H. Endou, Heterodimeric amino acid transporters: molecular biology and pathological and pharmacological relevance, Curr. Drug Metab. 2 (2001) 339–354.
[10] Y. Kanai, H. Segawa, K. Miyamoto, H. Uchino, E. Takeda, H. Endou, Expression cloning and characterization of a transporter for large neutral amino acids activated by the heavy chain of 4F2 antigen (CD98), J. Biol. Chem. 273 (1998) 23629–23632.
[11] O. Yanagida, Y. Kanai, A. Chairoungdua, D.K. Kim, H. Segawa, T. Nii, et al., Human L-type amino acid transporter 1 (LAT1): characterization of function and expression in tumor cell lines, Biochim. Biophys. Acta 1514 (2001) 291–302.
[12] H. Uchino, Y. Kanai, D.K. Kim, M.F. Wempe, A. Chairoungdua, E. Morimoto, M.W. Anders, H. Endou, Transport of amino acid-related compounds mediated by L-type amino acid transporter 1 (LAT1): insights into the mechanisms of substrate recognition, Mol. Pharmacol. 61 (2002) 729–737.
[13] B.A. Mannion, T.V. Kolesnikova, S.-H. Lin, N.L. Thompson, M.E. Hemler, The light chain of CD98 is identified as E16/TA1 protein, J. Biol. Chem. 273 (1998) 33127–33129.
[14] L. Mastroberardino, B. Spindler, R. Pfeiffer, P.J. Skelly, J. Loffing, C.B. Shoemaker, F. Verrey, Amino-acid transport by heterodimers of 4F2hc/CD98 and members of a permease family, Nature 395 (1998) 288–291.
[15] R. Pfeiffer, B. Spindler, J. Loffing, P.J. Skelly, C.B. Shoemaker, F. Verrey, Functional heterodimeric amino acid transporters lacking cysteine residues involved in disulfide bond, Fed. Eur. Biochem. Sci. Lett. 439 (1998) 157–162.
[16] E. Nakamura, M. Sato, H. Yang, F. Miyagawa, M. Harasaki, K. Tomita, et al., 4F2 (CD98) heavy chain is associated covalently with an amino acid transporter and controls intracellular trafficking and membrane topology of 4F2 heterodimer, J. Biol. Chem. 274 (1999) 3009–3016.
[17] P.D. Prasad, H. Wang, H. Huang, R. Kekuda, D.P. Rajan, F.H. Leibach, V. Ganapathy, Human LAT1, a subunit of system L amino acid transporter: molecular cloning and transport function, Biochem. Biophys. Res. Commun. 255 (1999) 283–288.
[18] J. Sang, Y.-P. Lim, M. Panzia, P. Finch, N.L. Thompson, TA1, a highly conserved oncofetal complementary DNA from rat hepatoma, encodes an integral membrane protein associated with liver development, carcinogenesis, and cell activation, Cancer Res. 55 (1995) 1152–1159.
[19] D.A. Wolf, S. Wang, M.A. Panzia, N.H. Bassily, N.L. Thompson, Expression of a highly conserved oncofetal gene, TA1/E16, in human colon carcinoma and other primary cancers: homology to *Schistosoma mansoni* amino acid permease and *Caenorhabditis elegans* gene products, Cancer Res. 56 (1996) 5012–5022.
[20] M. Pineda, E. Fernandez, D. Torrents, R. Estevez, C. Lopez, M. Camps, et al., Identification of a membrane protein, LAT-2, that co-expresses with 4F2 heavy chain, an L-type amino acid transport activity with broad specificity for small and large zwitterionic amino acids, J. Biol. Chem. 274 (1999) 19738–19744.
[21] G. Rossier, C. Meier, C. Bauch, V. Summa, B. Sordat, F. Verrey, L.C. Kuhn, LAT2, a new basolateral 4F2hc/CD98-associated amino acid transporter of kidney and intestine, J. Biol. Chem. 274 (1999) 34948–34954.
[22] H. Segawa, Y. Fukasawa, K. Miyamoto, E. Takeda, H. Endou, Y. Kanai, Identification and functional characterization of a Na^+-independent neutral amino acid transporter with broad substrate selectivity, J. Biol. Chem. 274 (1999) 19745–19751.
[23] D.P. Rajan, R. Kekuda, W. Huang, L.D. Devoe, F.H. Leibach, P.D. Prasad, V. Ganapathy, Cloning and functional characterization of a Na^+-independent, broad-specific neutral amino acid transporter from mammalian intestine, Biochim. Biophys. Acta 1463 (2000) 6–14.
[24] D.K. Kim, Y. Kanai, H.W. Choi, S. Tangtrongsup, A. Chairoungdua, E. Babu, et al., Characterization of the system L amino acid transporter in T24 human bladder carcinoma cells, Biochim. Biophys. Acta 1565 (2002) 112–121.
[25] P.N. Notani, Epidemiology and prevention of head and neck cancer: a global view, in: D. Saranath (Ed.), Contemporary

Issues in Oral Cancer, 2000, Oxford University Press, New Delhi, 2000, pp. 1–29.
[26] Y.S. Keum, J. Kim, K.H. Lee, K.K. Park, Y.J. Surh, J.M. Lee, et al., Induction of apoptosis and caspase-3 activation by chemopreventive [6]-paradol and structurally related compounds in KB cells, Cancer Lett. 177 (2002) 41–47.
[27] N. Utsunomiya-Tate, H. Endou, Y. Kanai, Cloning and functional characterization of a system ASC-like Na^+-dependent neutral amino acid transporter, J. Biol. Chem. 271 (1996) 14883–14890.
[28] D.E. Birch, Simplified hot start PCR, Nature 381 (1996) 445–446.
[29] D.K. Kim, Y. Kanai, H. Matsuo, J.Y. Kim, A. Chairoungdua, Y. Kobayashi, et al., The human T-type amino acid transporter-1: characterization, gene organization, and chromosomal location, Genomics 79 (2002) 95–103.
[30] N. Utsunomiya-Tate, H. Endou, Y. Kanai, Tissue specific variants of glutamate transporter GLT-1, Fed. Eur. Biochem. Sci. Lett. 416 (1997) 312–316.
[31] Y. Kanai, M.A. Hediger, Primary structure and functional characterization of a high-affinity glutamate transporter, Nature 360 (1992) 467–471.
[32] C.S.K. Mayanil, D. George, L. Freilich, E.J. Miljan, B. Mania-Farnell, D.G. McLone, E.G. Bremer, Microarray analysis detects novel Pax3 downstream target genes, J. Biol. Chem. 276 (2001) 49299–49309.
[33] B. Thorens, H.K. Sarkar, H.R. Kaback, H.F. Lodish, Cloning and functional expression in bacteria of a novel glucose transporter present in liver, intestine, kidney, and beta-pancreatic islet cells, Cell 55 (1988) 281–290.
[34] A. Chairoungdua, H. Segawa, J.Y. Kim, K. Miyamoto, H. Haga, Y. Fukui, et al., Identification of an amino acid transporter associated with the cystinuria-related type II membrane glycoprotein, J. Biol. Chem. 274 (1999) 28845–28848.
[35] Y. Fukasawa, H. Segawa, J.Y. Kim, A. Chairoungdua, D.K. Kim, H. Matsuo, et al., Identification and characterization of a Na^+-independent neutral amino acid transporter that associates with the 4F2 heavy chain and exhibits substrate selectivity for small neutral D- and L-amino acids, J. Biol. Chem. 275 (2000) 9690–9698.
[36] D.K. Kim, Y. Kanai, A. Chairoungdua, H. Matsuo, S.H. Cha, H. Endou, Expression cloning of a Na^+-independent aromatic amino acid transporter with structural similarity to H^+/monocarboxylate transporters, J. Biol. Chem. 276 (2001) 17221–17228.
[37] H. Ohkame, H. Masuda, Y. Ishii, Y. Kanai, Expression of L-type amino acid transporter 1 (LAT1) and 4F2 heavy chain (4F2hc) in liver tumor lesions of rat models, J. Surg. Oncol. 78 (2001) 265–271.
[38] H. Matsuo, S. Tsukada, T. Nakata, A. Chairoungdua, D.K. Kim, S.H. Cha, et al., Expression of a system L neutral amino acid transporter at the blood-brain barrier, NeuroReport 11 (2000) 3507–3511.
[39] K. Mizoguchi, S.H. Cha, A. Chairoungdua, D.K. Kim, Y. Shigeta, H. Matsuo, et al., Human cystinuria-related transporter: localization and functional characterization, Kidney Int. 59 (2001) 1821–1833.
[40] R. Todd, R.B. Donoff, D.T. Wong, The molecular biology of oral carcinogenesis: toward a tumor progression model, J. Oral. Maxillofac. Surg. 55 (1997) 613–623.
[41] H.N. Christensen, M.E. Handlogten, I. Lam, H.S. Tager, R. Zand, A bicyclic amino acid to improve discriminations among transport systems, J. Biol. Chem. 244 (1969) 1510–1520.
[42] J.L. Sloan, S. Mager, Cloning and functional expression of a human Na^+ and Cl^--dependent neutral and cationic amino acid transporter $B^{0,+}$, J. Biol. Chem. 274 (1999) 23740–23745.

Anat. Histol. Embryol. 33, 119–124 (2004)

ISSN 0340–2096

Oral Biology Research Institute, College of Dentistry, Chosun University, Gwang-ju, Korea

Preferential Expression of L-type Amino Acid Transporter 1 in Ameloblasts During Rat Tooth Development

J.-C. Park[1,2], Y. B. Kim[1], J. H. Yoon[1], H.-J. Kim[1], S. M. Kim[1], Y. Kanai[3], H. Endou[3] and D. K. Kim[1]*

Addresses of authors: [1]Oral Biology Research Institute, College of Dentistry, Chosun University, 375 Seo-Suk Dong, Dong-ku, Gwang-ju, 501-759, Korea; [2]Research Center for Proteineous Materials, Chosun University, 375 Seo-Suk Dong, Dong-ku, Gwang-ju, 501-759, Korea; [3]Department of Pharmacology and Toxicology, Kyorin University School of Medicine, 6-20-2 Shinkawa, Tokyo 181-8611, Japan; *Corresponding author: Tel.: +82-62-230-6893; fax: +82-62-223-3205; e-mail: kdk@chosun.ac.kr

With 9 figures

Received June 2003; accepted for publication September 2003

Summary

Certain amino acid transport systems play an important role in supplying organic nutrients to each cell and for cell proliferation during tooth development. However, the mechanisms responsible for such actions are unclear. This study demonstrated for the first time that LAT1 and 4F2hc are expressed during tooth development in prenatal and postnatal rats, and that the transporters show cell-specific expression in ameloblasts, which are the epithelium-derived dental cells. LAT1 and 4F2hc expression was not observed in other dental cells of the developing teeth such as odontoblasts and cementoblasts. Overall, these results suggest that LAT1 and 4F2hc might play an important role in enamel formation.

Introduction

Tooth development in mammals and other vertebrates is a multistage and multistep process involving the determination and patterning events, the epithelial–mesenchymal interactions and cell migration, proliferation, and differentiation (Slavkin and Diekwisch, 1996; Thesleff and Sharp, 1997; Yoshiba et al., 1998; Shimo et al., 2002). Among the many events and processes involved in odontogenesis, little is known regarding the amino acid transport system that supplies nutrients despite the significant roles in initiating tooth germ formation and in sustaining differentiation and maturation of the dental structures.

Recently, various members of a novel family of glycoprotein-associated amino acid transporters were identified and were shown to play important roles in cellular uptake and/or basolateral extrusion of basic and neutral amino acids (Kanai et al., 2000). System L is a plasma membrane amino acid transporter, which mediates the Na^+-independent transport of large neutral amino acids (Oxender and Christensen, 1963; Christensen, 1990; Kim et al., 2002). Using expression cloning, L-type amino acid transporter 1 (LAT1) was isolated as the first isoform of the system L amino acid transporter from the C6 rat glioma cells by Kanai et al. (1998). It was further demonstrated that a single-membrane spanning protein, the heavy chain of the 4F2 antigen (4F2hc), is essential for the functional expression of LAT1 (Mannion et al., 1998; Kanai and Endou, 2001; Ohkame et al., 2001; Okamoto et al., 2002). LAT1 and 4F2hc form a heterodimeric complex via a disulphide bond. Although 4F2hc expression is ubiquitous, LAT1 expression is restricted to certain tissues such as cultured cells and malignant tumours, presumably to support their continuous growth.

In developing teeth, the developmental expression pattern of amino acid transporter has not yet been analysed. This study characterized the changes in localization of LAT1 and 4F2hc during rat tooth development using immunohistochemistry.

Materials and Methods

Animal and tissue preparation

All animal experiments were approved by the Review Committee on the Use of Experimental Animals and Human Subjects (Chosun University, Gwang-ju, Korea) prior to the experiments. Sprague–Dawley rats at embryonic days 16, 18 (E 16, E 18), and postnatal days 2, 7, 14, 21, 28 and 41 (PN 2, PN 7, PN 14, PN 21, PN 28, PN 41) were used in this study (MacNeil et al., 1998; Mistry et al., 2001; Onishi et al., 2002). The animals were perfused transcardially with a solution containing 4% paraformaldehyde in phosphate-buffered saline (PBS; pH 7.4) for 20 min. The maxillae and mandibles were dissected out, post-fixed in 4% paraformaldehyde in PBS (pH 7.4) at 4°C for 16 h, and decalcified with 10% ethylene diamine tetraacetic acid (EDTA) at 4°C for 4 weeks. All the specimens were routinely embedded in paraffin, after cutting in 5-μm thickness, mounted on ethoxysilran-coated slides and stored at 4°C until needed for immunochemical staining.

Immunohistochemistry

The paraffin sections were deparaffinized with xylene and rehydrated with serial alcohols. Each section was washed twice with PBS, and the endogenous peroxidase was blocked by placing the section in a buffer solution of methanol containing 0.3% hydrogen peroxide for 20–30 min. The sections were washed three times with PBS. The sections were incubated in a PBS solution containing 0.5% bovine serum albumin (BSA) for 20 min and then washed with PBS. The sections were incubated overnight at 4°C with the primary antibodies (rat anti-LAT1, 1 : 200; rat anti-4F2hc, 1 : 200; Kumamoto Immunochemical Lab, Transgenic, Kumamoto,

U. S. Copyright Clearance Center Code Statement: 0340–2096/2004/3302–0119$15.00/0

Japan). After washing with PBS for 40 min, the sections were incubated with biotinylated goat anti-rat IgG antibodies (Vector Lab, Burlingame, CA, USA) diluted with PBS containing 0.5% BSA as the secondary antibody at room temperature for 1 h. After washing for 20 min with PBS, the sections were reacted with avidine–biotin–peroxidase complex (ABC) reagent (Vector Lab) for 45 min. After washing for 20 min in PBS, the section was developed using 0.05% diaminobenzidine tetrahydrochloride (DAB; Dako Corp., Capinteria, CA, USA). The sections were then washed, counterstained with haematoxylin and observed using optical microscopy.

Results

This study focused on determining the expression level of LAT1 and the 4F2hc amino acid transporters during tooth development in rats, i.e. from embryonic day 16 to postnatal day 41.

Bud and cap stages (E 18)

At E 18, the oral epithelium was invaginated and formed the tooth bud. The tooth bud began to further differentiate into a dental organ, dental papilla and surrounding dental follicle. 4F2hc was expressed in the tooth bud and the dental organ (Fig. 1), while LAT1 expression was not detected in either the tooth bud or the dental organ (Fig. 2).

Crown stage (PN 7)

At PN 7, when the dentine and enamel had been mineralized, 4F2hc expression was observed in only the functional ameloblasts (Fig. 3), while the LAT1 was expressed in the functional ameloblasts, tooth follicles and the surrounding alveolar bone (Fig. 4). LAT1 and 4F2hc expression was not detected in the odontoblasts of the developing pulp.

Root formation and periodontal ligament alignment stage (PN 14)

At PN 14, root formation was almost complete. The periodontal ligament was organized and inserted perpendicularly into the cemental surface of the root. During root formation and periodontal ligament alignment, LAT1 was localized in the ameloblasts, the adjacent dental organ derivatives, the developing periodontal ligament, and the alveolar bone, whereas 4F2hc was still expressed in the ameloblasts only (Figs 5–8). LAT1 and 4F2hc expression was not detected in odontoblasts and cementoblasts of the developing teeth.

Erupted and functional stages of posterior tooth (PN 41)

At PN 41, the molar tooth had fully erupted and attained a functional occlusion. At the functional stage of the teeth, LAT1 and 4F2hc expression were not detected in any of the

Fig. 1. 4F2hc immunostaining of the bud and cap stages of the rat tooth germs (E 18). 4F2hc immunoreactivity is detected in the tooth bud (tb) and epithelial dental organ (do), ×100.

Fig. 2. LAT1 immunostaining of the bud and cap stages of the rat tooth germs (E 18). Tooth germs show no LAT1 immunostaining, ×100.

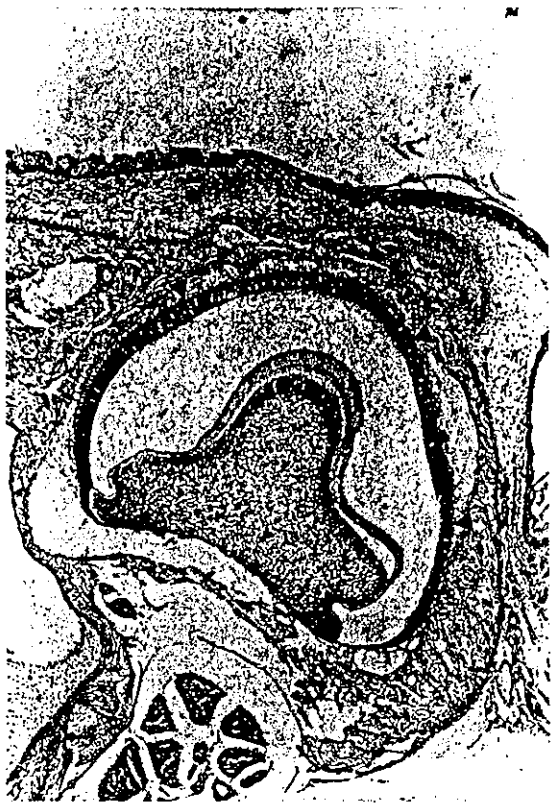

Fig. 3. 4F2hc immunostaining of the crown stage of a rat tooth (PN 7). 4F2hc immunoreactivity can be seen in the ameloblasts (arrowheads), ×40.

Fig. 5. 4F2hc immunostaining of the root formation stage of a rat tooth (PN 14). 4F2hc expression can be seen in the ameloblasts, ×40.

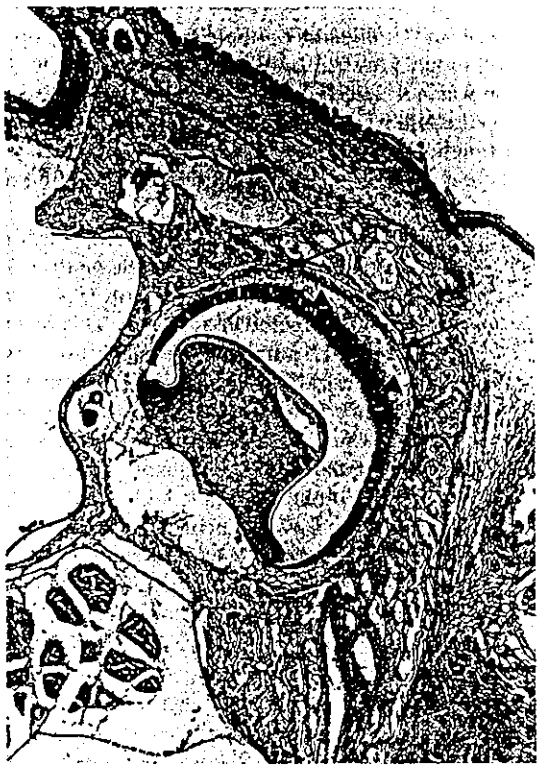

Fig. 4. LAT1 immunostaining of the crown stage of a rat tooth (PN 7). LAT1 expression can be observed in the ameloblasts (arrowheads), tooth follicle (arrows), and surrounding alveolar bone, ×40.

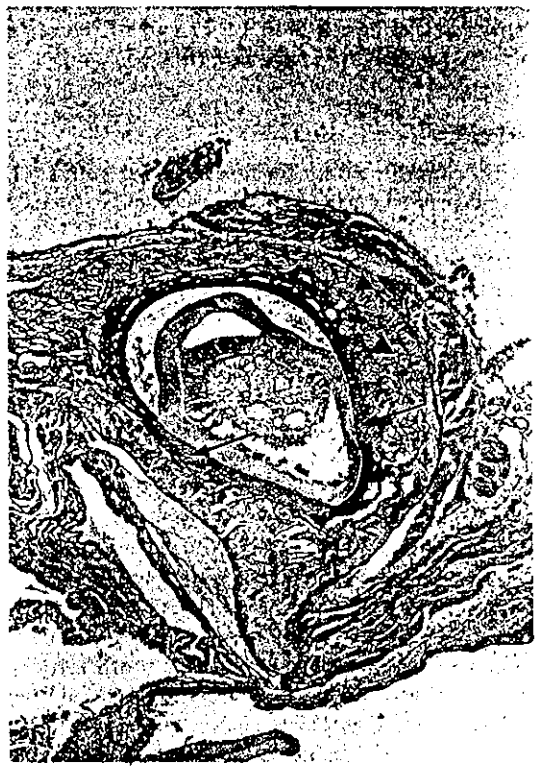

Fig. 6. LAT1 immunostaining of the root formation stage of a rat tooth (PN 14). LAT1 expression is detected in the ameloblasts, the developing periodontal ligament (arrows), and the surrounding alveolar bone (arrowheads), ×40.

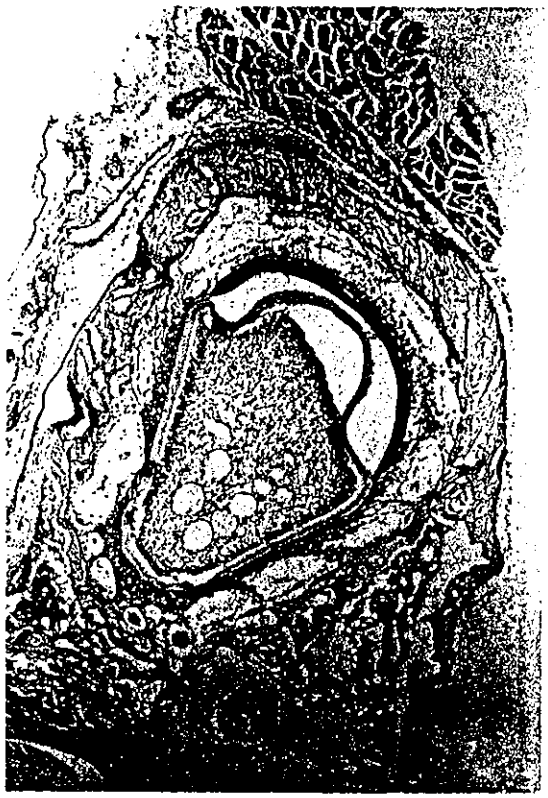

Fig. 7. 4F2hc immunostaining of the root formation and periodontal ligament alignment stage of a rat tooth (PN 14). 4F2hc immunoreactivity can be observed in only the ameloblasts, ×40.

Fig. 8. LAT1 immunostaining of the root formation and periodontal ligament alignment stage of a rat tooth (PN 14). LAT1 immunoreactivity can be seen in the ameloblasts, adjacent dental organ derivatives, and alveolar bone (arrowheads). LAT1 expression can also be observed in the developing periodontal ligament (arrows), ×40.

tooth structures, although both LAT1 and 4F2hc expression were observed in the oral epithelium (Fig. 9).

Discussion

This study demonstrated for the first time that both LAT1 and 4F2hc are expressed during tooth development in prenatal and postnatal rats. In addition, this study showed that the transporters exhibit cell-specific expression in ameloblasts, which are the epithelium-derived dental cells. LAT1 and 4F2hc expression was not observed in the odontoblasts and cementoblasts of the developing teeth. Such results can be caused by the amino acid composition of the enamel being different from those of the dentine and cementum. The enamel protein consists of a relatively high concentration of proline, glutamic acid, leucine and histidine, but dentine and cementum proteins are composed of proline, glycine, alanine, aspartic acid and arginine (Glimcher, 1971; Gallop et al., 1972). The LAT1 transporter prefers large neutral amino acids such as leucine, isoleucine, valine, phenylalanine, tyrosine, tryptophan, methionine and histidine for its substrates (Kanai et al., 1998; Yanagida et al., 2001; Uchino et al., 2002). The ameloblasts are unique epithelium-derived cells in the tooth forming cells and show relatively higher cell growth potential than the odontoblasts and cementoblasts. Christensen (1990) revealed that LAT1 is present in the basolateral membrane of the epithelial cells and plays an important role in the absorption of amino acids through the epithelial cells of the small intestine and renal proximal tubules. Another report (Yanagida et al., 2001) also showed that LAT1 is highly expressed in the cultured cell and malignant tumours, presumably supporting their continuous growth. In this study, 4F2hc and LAT1 expression was not detected in any tooth structures except for the oral epithelium when the molar tooth has fully erupted and attained functional occlusion. In truth, this is caused by the fact that the ameloblasts are not present in the fully erupted functional teeth.

System L is a major nutrient transport system responsible for the Na^+-independent transport of large neutral amino acids including several essential amino acids (Kanai et al., 1998; Segawa et al., 1999; Uchino et al., 2002). This permease-related protein contains 12 putative transmembrane domains and requires heterodimerization with a type II transmembrane heavy-chain protein such as 4F2hc to express their function as transporters. LAT1, which is the first isoform of the system L transporter, is up-regulated in malignant tumour, which provides evidence of tumour growth. LAT1 also requires an additional protein 4F2hc for its functional expression (Verry et al., 2000; Bröer et al., 2001; Yanagida et al., 2001). The 4F2hc cell surface antigen is a 120-kDa disulphide-linked heterodimer composed of an 80-kDa heavy chain and a 40-kDa light chain. The 4F2 antigen was originally identified as a lymphocyte activation antigen, but little is known regarding its function. It has been shown that LAT1, LAT2, y^+LAT1, y^+LAT2 and cystine transporter xCT are linked to 4F2hc. The results show that 4F2hc is expressed in the early developmental stages of the teeth, bud and cap stages of tooth development, but LAT1 appears at the latter stage, bell stage. Although 4F2hc expression is ubiquitous, LAT1 expression is

Fig. 9. LAT1 immunostaining of the functional rat tooth (PN 41). LAT1 expression has disappeared in periodontal ligament and other tooth structures, ×40.

restricted to certain tissues (Kanai et al., 1998; Yanagida et al., 2001). Mathias et al. (2001) revealed that the ameloblast, which is a highly specialized multifunctional cell, regulates the production and transport of proteins into the extracellular matrix of enamel. The nature and behaviour of the enamel proteins are longstanding and intriguing questions (Zeichner-David et al., 1997; Ravindranath et al., 2001). In the developing dental organ, the inner dental epithelium differentiates into presecretory ameloblasts, secretory ameloblasts and ultimately into mature ameloblasts. The secretory ameloblast is involved not only in the synthesis, secretion and resorption of enamel proteins, but is also involved in the active transport of Ca^{2+} into the extracellular matrix. During the maturation process, ameloblast cells change their morphology from ruffled-ended ameloblasts to smooth-ended ameloblasts. These mature ameloblasts act as regulatory and transporting cells, and to modulate the latter stages of the mineralization process. It is believed that LAT1 is expressed in the initial stage of tooth development corresponding to the bell/advanced bell stage. In addition, more amino acid supplies are needed in the secretory and maturation ameloblasts compared with the presecretory ameloblasts.

During periodontal ligament alignment, LAT1 is localized in the ameloblasts, the adjacent dental organ derivatives, the alveolar bone and the developing periodontal ligament, whereas 4F2hc was present only in the ameloblasts. These results suggest that LAT1 may interact with other unknown factors in alveolar bone and periodontal ligament development but not with 4F2hc. The dental organ derivatives have an epithelial origin and consist of the inner dental epithelium, the outer dental epithelium, the stellate reticulum and the stratum intermedium.

No LAT1 expression could be found in the alveolar bone and periodontal ligament of the fully erupted functional teeth, which suggests that there is no active exchange of amino acids in the mature alveolar bone and periodontal ligament. However, there is the possibility that other amino acid transporters may be involved in the maintenance of mature alveolar bone and the periodontal ligament.

In conclusion, these results suggest that LAT1 and 4F2hc play an important role in enamel formation. Further studies aimed at determining the role of other amino acid transporters such as the basic, acidic and neutral amino acid transporters during tooth development are currently underway.

Acknowledgements

This study was supported by Research funds from Chosun University, 2001. Anti-LAT1 and its blocking peptide were supplied by Kumamoto Immunochemical Laboratory, Transgenic, Kumamoto, Japan.

References

Bröer, A., B. Friedrich, C. A. Wagner, S. Fillon, V. Ganapathy, F. Lang, and S. Bröer, 2001: Association of 4F2hc with light chains LAT1, LAT2, or y^+LAT2 requires different domains. Biochem. J. **355,** 725–731.

Christensen, H. N., 1990: Role of amino acid transport and counter-transport in nutrition and metabolism. Physiol. Rev. **70,** 43–77.

Gallop, P. M., O. O. Blumenfeld, and S. Seifter, 1972: Structure and metabolism of connective tissue proteins. Ann. Rev. Biochem. **41,** 617–672.

Glimcher, M. J., 1971: Studies of the Proteins of Embryonic and Mature Dental Enamel; The Enamelins, Chemistry and Physiology of Enamel. Michigan, MI: University of Michigan Symposium.

Kanai, Y., and H. Endou, 2001: Heterodimeric amino acid transporters: molecular biology and pathological and pharmacological relevance. Curr. Drug Metab. **2,** 339–354.

Kanai, Y., H. Segawa, K.-I. Miyamoto, H. Uchino, E. Takeda, and H. Endou, 1998: Expression cloning and characterization of a transporter for large neutral amino acids activated by the heavy chain of 4F2 antigen (CD98). J. Biol. Chem. **273,** 23629–23632.

Kanai, Y., Y. Fukasawa, S. H. Cha, H. Segawa, A. Chairoungdua, D. K. Kim, H. Matsuo, J. Y. Kim, K. Miyamoto, E. Takeda, and H. Endou, 2000: Transport properties of a system y^+L neutral and basic amino acid transporter. Insights into the mechanisms of substrate recognition. J. Biol. Chem. **275,** 20787–20793.

Kim, D. K., Y. Kanai, H. W. Choi, S. Tangtrongsup, A. Chairoungdua, E. Babu, K. Tachampa, N. Anzai, Y. Iribe, and H. Endou, 2002: Characterization of the system L amino acid transporter in T24 human bladder carcinoma cells. Bioch. Biophy. Acta **1565,** 112–122.

MacNeil, R. L., J. E. Berry, C. L. Strayhorn, Y. Shigeyama, and M. J. Sommerman, 1998: Expression of type I and type XII collagen during development of the periodontal ligament in the mouse. Arch. Oral Biol. **43,** 779–787.

Mannion, B. A., T. V. Kolesnikova, S.-H. Lin, N. L. Thompson, and M. E. Hemler, 1998: The light chain of CD98 is identified as E16/TA1 protein. J. Biol. Chem. **273,** 33127–33129.

Mathias, R. S., C. H. E. Mathews, C. Gao, D. Machule, W. Li, and P. K. Denbesten, 2001: Identification of the calcium-sensing receptor in the developing tooth organ. J. Bone Min. Res. **16,** 2238–2244.

Mistry, D., M. Altini, H. G. Coleman, H. Ali, and E. Maiorano, 2001: The spatial and temporal expression of calretinin in developing rat molars (*Rattus norvegicus*). Arch. Oral. Biol. **46,** 973–981.

Ohkame, H., H. Masuda, Y. Ishii, and Y. Kanai, 2001: Expression of L-type amino acid transporter (LAT1) and 4F2hc heavy chain (4F2hc) in liver tumor lesion of rat models. J. Surg. Oncol. **78,** 265–272.

Okamoto, Y., M. Sakata, K. Ogura, T. Yamamoto, M. Yamaguchi, K. Tasaka, H. Kurachi, M. Tsurudome, and Y. Murata, 2002: Expression and regulation of 4F2hc and hLAT1 in human trophoblasts. Am. J. Physiol. Cell Physiol. **282,** 196–204.

Onishi, T., H. Tsubone, T. Ooshima, S. Sobue, A. El-Sharaby, and S. Wakisaka, 2002: Immunohistochemical localization of heat shock protein 25 (HSP 25) during root formation of rat molar. Anat. Rec. **267,** 321–329.

Oxender, D. L., and H. L. Christensen, 1963: Evidence for two types of mediation of neutral amino acid transport in Ehrlich cells. Nature **197,** 765–767.

Ravindranath, R. M., W.-Y. Tam, P. Bringas, V. Santos, and A. G. Fincham, 2001: Amelogenin–cytokeratin 14 interaction in ameloblasts during enamel formation. J. Biol. Chem. **276,** 36586–36597.

Segawa, H., Y. Fukasawa, K.-I. Miyamoto, E. Takeda, H. Endou, and Y. Kanai, 1999: Identification and functional characterization of a Na^+-independent neutral amino acid transporter with broad substrate selectivity. J. Biol. Chem. 19745–19751.

Shimo, T., C. Wu, P. C. Billings, R. Piddington, J. Rosenbloom, M. Pacifini, and E. Koyama, 2002: Expression, gene regulation, and roles of Fisp/CTGF in developing tooth germs. Dev. Dyn. **224,** 267–278.

Slavkin, H., and T. Diekwisch, 1996: Evolution in tooth developmental biology of morphology and molecules. Anat. Rec. **245,** 131–150.

Thesleff, I., and P. Sharp, 1997: Signaling networks regulating dental development. Mech. Dev. **67,** 111–123.

Uchino, H., Y. Kanai, D. K. Kim, M. F. Wempe, A. Chairoungdua, E. Morimoto, M. W. Anders, and H. Endou, 2002: Transport of amino acid-related compounds mediated by L-type amino acid transporter 1 (LAT1): insights into the mechanisms of substrate recognition. Mol. Pharmacol. **61,** 729–737.

Verry, F., C. Meier, G. Rossier, and L. C. Kühn, 2000: Glycoprotein-associated amino acid exchangers: broadening the range of transport specificity. Pflügers Arch-Eur. J. Physiol. **440,** 503–512.

Yanagida, O., Y. Kanai, A. Chairoungdua, D. K. Kim, H. Segawa, T. Nii, H. S. Cha, H. Matsuo, J.-I. Fukushima, Y. Fukasawa, Y. Tani, Y. Takatani, H. Uchino, J. Y. Kim, J. Inatomi, I. Okayasu, K.-I. Miyamoto, E. Takeda, T. Goya, and H. Endou, 2001: Human L-type amino acid transporter 1 (LAT1): characterization of function and expression in tumor cell lines. Bioch. Biophy. Acta **1514,** 291–302.

Yoshiba, K., N. Yoshiba, D. Aberdam, G. Meneguzzi, F. Perrin-Schmitt, C. Stoetzel, J. V. Ruch, and H. Lesot, 1998: Expression and localization of laminin-5 subunits during mouse tooth development. Dev. Dyn. **211,** 164–176.

Zeichner-David, M., J. Vo, H. Tan, T. Diekwisch, B. Berman, F. Thiemann, M. D. Alcocer, P. Hse, T. Wang, J. Eyna, J. Caton, H. C. Slavkin, and M. MacDougall, 1997: Timing of the expression of enamel gene products during mouse tooth development. Int. J. Dev. Biol. **41,** 27–38.

THE JOURNAL OF BIOLOGICAL CHEMISTRY
Vol. 279, No. 44, Issue of October 29, pp. 45942–45950, 2004
Printed in U.S.A.

The Multivalent PDZ Domain-containing Protein PDZK1 Regulates Transport Activity of Renal Urate-Anion Exchanger URAT1 via Its C Terminus*

Received for publication, June 16, 2004, and in revised form, August 2, 2004
Published, JBC Papers in Press, August 10, 2004, DOI 10.1074/jbc.M406724200

Naohiko Anzai‡§, Hiroki Miyazaki‡§¶, Rie Noshiro‡, Suparat Khamdang‡, Arthit Chairoungdua‡, Ho-Jung Shin‡, Atsushi Enomoto‡, Shinichi Sakamoto‡, Taku Hirata‡, Kimio Tomita¶, Yoshikatsu Kanai‡, and Hitoshi Endou‡‖

From the ‡Department of Pharmacology and Toxicology, Kyorin University School of Medicine, 6-20-2, Shinkawa, Mitaka-shi, Tokyo 181-8611 and the and ¶Department of Nephrology, Graduate School of Medical Sciences, Kumamoto University, 1-1-1, Honjo, Kumamoto-shi, Kumamoto 860-8556, Japan

The urate-anion exchanger URAT1 is a member of the organic anion transporter (OAT) family that regulates blood urate level in humans and is targeted by uricosuric and antiuricosuric agents (Enomoto, A., Kimura, H., Chairoungdua, A., Shigeta, Y., Jutabha, P., Cha, S. H., Hosoyamada, M., Takeda, M., Sekine, T., Igarashi, T., Matsuo, H., Kikuchi, Y., Oda, T., Ichida, K., Hosoya, T., Shimotaka, K., Niwa, T., Kanai, Y., and Endou, H. (2002) *Nature* 417, 447–452). URAT1 is expressed only in the kidney, where it is thought to participate in tubular urate reabsorption. We found that the multivalent PDZ (PSD-95, *Drosophila* discs-large protein, *Zonula occludens* protein 1) domain-containing protein, PDZK1 interacts with URAT1 in a yeast two-hybrid screen. Such an interaction requires the PDZ motif of URAT1 in its extreme intracellular C-terminal region and the first, second, and fourth PDZ domains of PDZK1 as identified by yeast two-hybrid assay, *in vitro* binding assay and surface plasmon resonance analysis (K_D = 1.97–514 nM). Coimmunoprecipitation studies revealed that the wild-type URAT1, but not its mutant lacking the PDZ-motif, directly interacts with PDZK1. Colocalization of URAT1 and PDZK1 was observed at the apical membrane of renal proximal tubular cells. The association of URAT1 with PDZK1 enhanced urate transport activities in HEK293 cells (1.4-fold), and the deletion of the URAT1 C-terminal PDZ motif abolished this effect. The augmentation of the transport activity was accompanied by a significant increase in the V_{max} of urate transport via URAT1 and was associated with the increased surface expression level of URAT1 protein from HEK293 cells stably expressing URAT1 transfected with PDZK1. Taken together, the present study indicates the novel role of PDZK1 in regulating the functional activity of URAT1-mediated urate transport in the apical membrane of renal proximal tubules.

Urate is the major inert end product of purine degradation in humans and higher primates in contrast to most other mammals because of the genetic silencing of hepatic oxidative enzyme uricase (1, 2). The kidney plays a dominant role in urate elimination; it excretes ~70% of the daily urate production. Urate exists primarily as a weak acid at physiological pH (pK_a 5.75), and most of it is dissociated in blood and is freely filtered through the glomerulus. Thus, urate enters the proximal tubule in its anionic form, but it hardly permeates the tubular cells in the absence of facilitated mechanisms owing to its hydrophilicity. The transport mechanisms for urate are localized in the proximal tubule. In humans, urate is almost completely reabsorbed, which results in the excretion of ~10% of its filtered load. The absence of uricase and the presence of an effective renal urate reabsorption system contribute to higher blood urate levels in humans. Therefore, it was postulated that defects in tubular urate transport cause hypouricemia and decreased renal urate clearance leads to hyperuricemia in most hyperuricemic patients (3).

Recently, we have identified the long hypothesized urate transporter in the human kidney (URAT1,[1] encoded by *SLC22A12*), a urate-anion exchanger localized on the apical side of the proximal tubule (4). URAT1 is targeted by uricosuric and antiuricosuric agents that affect urate excretion (*e.g.* benzbromarone, probenecid, and pyrazinamide). The pharmacological properties manifested by URAT1 cRNA-injected *Xenopus* oocytes are consistent with those of the previously described urate transport activities in human brush-border membrane vesicles. We also found that defects in *SLC22A12* lead to idiopathic renal hypouricemia (Mendelian Inheritance in Man number 220150), and patients with such defects show a high fractional urate excretion such as 95 ± 10% (normally <10%). These results indicate that URAT1 regulates blood urate level and *vice versa*, that is, to control blood urate levels, the URAT1 transport function should be regulated. A newly found genetic alteration in *SLC22A12* from a patient of an idiopathic renal hypouricemia has prompted us to consider the importance of the URAT1 extreme intracellular C-terminal region for its function (5). A 5-bp deletion near the URAT1 C-terminal end (1639–1643del) causes frameshift, and the seven amino acids

* This work was supported in part by grants from the Japanese Ministry of Education Science, Sports, Culture and Technology, grants-in-aid for Scientific Research and Bioventure Project from the Science Research Promotion Fund of the Japan Private School Promotion Foundation, and grants-in-aid from the Tokyo Biochemical Research Foundation. The costs of publication of this article were defrayed in part by the payment of page charges. This article must therefore be hereby marked "*advertisement*" in accordance with 18 U.S.C. Section 1734 solely to indicate this fact.

§ Both authors contributed equally to this work.

‖ To whom correspondence should be addressed. Tel.: 81-422-47-5511 (ext. 3451); Fax: 81-422-79-1321; E-mail: endouh@kyorin-u.ac.jp.

[1] The abbreviations used are: URAT1, urate-anion exchanger 1; OAT, organic anion transporter; GST, glutathione *S*-transferase; PDZ, PSD-95/Dlg/ZO-1 homology domain; NHERF, Na^+/H^+-exchanger regulatory factor; CT, C terminus; wt, wild type; PBS, phosphate-buffered saline; GFP, green fluorescent protein; HEK, human embryonic kidney; MBP, maltose binding protein; SPR, surface plasmon resonance; IKEPP, intestinal and kidney-enriched PDZ protein.

in the terminal sequences have changed into eight different amino acids. The URAT1 transport activity of this mutation is low in the *Xenopus* oocyte expression system. Interestingly, the PDZ binding motif at the C-terminal end of URAT1, which is known to participate in protein-protein interaction, disappears by this amino acid sequence modification.

PDZ (PSD-95, DglA, and ZO-1)-binding domains have been identified in various proteins and are known to be modular protein-protein recognition domains that play a role in protein targeting and protein complex assembly (6–8). These domains range from 80 to 90 amino acids in length and bind typically to proteins containing the tripeptide motif (S/T)*X*Ø (X = any amino acid and Ø = a hydrophobic residue) at their C termini (9, 10). These multidomain molecules not only target and provide scaffolds for protein-protein interactions but also modulate the function of receptors and ion channels, by which they associate (11–16). The disruption of the association between PDZ proteins and their targets contributes to the pathogenesis of a number of human diseases, most probably because of the failure of PDZ proteins to appropriately target and modulate the actions of associated proteins (6).

In this study, we use the yeast two-hybrid approach to investigate the putative URAT1-associated proteins that modulate its transport function. We identify the multivalent PDZ domain-containing protein PDZK1 as an apparent partner of URAT1 in the human kidney. Moreover, we show a functional consequence of PDZK1-URAT1 interaction in transfected HEK293 cells, where URAT1 transport activities were increased by 1.4-fold by coexpression of PDZK1. We speculate that PDZK1 is a scaffolding protein that may be a physiological regulator of the function of URAT1.

EXPERIMENTAL PROCEDURES

Plasmid Construction—The C-terminal fragments of human URAT1 cDNA, comprising three mutants (designated as d3, F555A, and T553A), were generated by PCR (antisense primers, 5′-CTC TCG AGC TAA AAC TGT GTG GAT TTT A-3′, 5′-CCC TCG AGC TAG GAT TTT AGG ACA GAG TTC-3′, 5′-CCC TCG AGC TAA GCC TGT GTG GAT TTT AGG A-3′, and 5′-CCC TCG AGC TAA AAC TGT GCG GAT TTT A-3′, respectively; sense primer, 5′-CGA ATT CCT GCC CGA GAC CCA GAG-3′) and inserted into the EcoRI and XhoI sites of the pEG202 plasmid, a LexA DNA-binding domain fusion vector. The same human URAT1 C-terminal fragments were also inserted into the pGEX-6P-1 plasmid (Amersham Biosciences) for GST fusion protein production. The full-length coding sequences of human URAT1 (wt) as well as its C-terminal 3-amino acid deletion mutants (d3) were inserted into the mammalian expression plasmid pcDNA3.1 (Invitrogen) for functional analysis and into the pEGFP-C2 plasmid for EGFP-URAT1 (Clontech) fusion protein preparation. The full-length coding sequence of human PDZK1 (GenBank™ accession number NM_002614) was amplified from the Cap-site human kidney cDNA (Nippongene, Japan) and subcloned into pcDNA3.1, into the pJG4-5 plasmid and a B42 activation domain fusion vector. Prey vectors (pJG4-5 and pMAL-c2X (New England Biolabs) for MBP fusion protein preparation) containing a single one PDZ domain of human PDZK1 were generated by PCR (PDZ1: sense primer, 5′-CTG CAA TTG ATG ACC TCC ACC TTC AAC-3′, and antisense primer, 5′-CCC TCG AGC TAC TTC TGA CTT TGA CCC A-3′; PDZ2: sense primer, 5′-CGA ATT CCA GAA GGA GCA AGG TTT G-3′, and antisense primer, 5′-CCC TCG AGC TAT TTC AAA CTG GCT TC-3′; PDZ3: sense primer, 5′-CGA ATT CAA GCG TCA TGT TGA GCA G-3′, and antisense primer, 5′-CCC TCG AGC TAA GAA GTG GGA GTA GGA GC-3′; PDZ4: sense primer, 5′-CGA ATT CAA GGA GGC TCC AGC TCC-3′, and antisense primer, 5′-CGC TCG AGT CAC ATC TCT GTA TCT TC-3′). The sequences of all constructs were confirmed by automatic DNA sequencing (Applied Biosystems 3730xl Sequencer).

Library Construction and Yeast Two-hybrid Screen—A human kidney cDNA library was constructed as described previously (11). Briefly, human kidney poly(A)$^+$ RNA purchased from Clontech was used to produce cDNA using a cDNA synthesis kit (Stratagene) with modified oligo(dT) primers carrying an XhoI restriction site and EcoRI adaptors to allow unidirectional cloning in an appropriate vector. The cDNAs were then purified using a CHROMA SPIN-400 column (Clontech) to pool cDNAs of 0.5 kb or longer, and ligated into the pJG4-5 prey vector previously digested with EcoRI and XhoI. After transformation in bacteria, 2.1×10^6 independent clones were obtained. Sixteen clones were randomly picked and digested with EcoRI and XhoI; all of them contained inserts with an average size of 1.3 kb (ranging from 0.5 to more than 3 kb).

A URAT1 C-terminal bait corresponding to the last 39 amino acids of URAT1 was used to screen 1.8×10^7 clones of the human kidney cDNA library with the LexA-based GFP two-hybrid system (Grow'n'Glow system; MoBiTec). Several positive clones were obtained and confirmed in a second round of screening using the yeast system. The expression of all the bait constructs in yeast was confirmed by Western blot analysis of yeast protein extracts using an anti-LexA antibody (Santa Cruz Biotechnology) (data not shown).

GST Fusion Protein Binding Assay—The URAT1 intracellular C-terminal region used as bait in the two-hybrid screen was inserted into the pGEX-6P-1 plasmid (Amersham Biosciences) for GST fusion protein production in bacteria as reported previously (11). Briefly, the bacterial pellet was resuspended in a sonication buffer (50 mM Tris-HCl (pH 8.0), 50 mM NaCl, 1 mM EDTA, and 1 mM dithiothreitol) and sonicated for 1 min. Triton X-100 (1% final) was added to the mixture, which was then centrifuged for 30 min at 15,000 rpm at 4 °C. The supernatant was used for protein binding assay.

Maltose binding protein (MBP), fused proteins consisting of PDZK1 individual PDZ domains were purified as described above. Then they were purified using a MagExtracter MBP fusion Protein Purification kit (TOYOBO, Osaka, Japan) according to the manufacturer's instructions.

In vitro translation was performed from a plasmid carrying the full-length PDZK1 preceded by a T7 promoter sequence with the TnT T7 Quick for PCR DNA system (Promega) in a final volume of 50 μl for 60 min at 30 °C in the presence of Transcend Biotinylated tRNA (Promega). 5 μl each of *in vitro*-translated products or of MBP fusion proteins was applied together with 50 μl of GST-glutathione-Sepharose resin to Handee Spin Cup columns using the ProFound Pull-Down GST Protein:Protein Interaction kit (Pierce), and protein complexes were eluted according to the manufacturer's instructions. The eluted samples were resuspended in Laemmli buffer, heated for 5 min at 95 °C, and electrophoresed in 10% SDS-PAGE gels; the fractionated proteins were blotted onto polyvinylidene difluoride membranes. The precipitated proteins were detected with the Transcend Chemiluminescent Translation Detection System (Promega) or immunoblotting using anti-MBP antiserum (New England Biolabs) developed by enhanced chemiluminescence.

Surface Plasmon Resonance—The interaction of URAT1 C terminus with individual PDZ domains of PDZK1 was investigated by the use of a BIAcore 3000 analytical system (BIAcore AB) based on principles described previously (17). URAT1 C-terminal fragment, referred to as the ligand, was immobilized on a sensor chip, and the interaction with PDZK1 individual PDZ domains fused with MBP, referred as the analytes, was detected through the mass changes of the reflective index on the sensor surface. All of the reagents such as an amine coupling kit, running buffer HBS-EP (0.01 M HEPES, pH 7.4, 0.15 M NaCl, 3 mM EDTA, 0.005% Surfactant P20), and the CM5 sensor chip were obtained from BIAcore AB. Using an amine coupling kit, GST-fused URAT1 CT wild-type or GST protein alone was attached to a CM5 sensor chip according to the manufacturer's instructions, giving a gain of 10,673 resonance units for GST-URAT1-CT or 8,566 resonance units for GST alone. Binding experiments were performed with the PDZK1 single one PDZ domains (PDZ1 to PDZ4) fused with MBP as described above. The analyte was injected at a flow rate of 30 μl/min in HBS-EP buffer at 25 °C, and the association and dissociation phases (upon switching back to buffer) were monitored for 120 and 180 s, respectively. For data acquisition, five different concentrations of each protein were used. At least two replicate experiments were performed for each fusion protein. Data were analyzed with the BIAevaluation program 3.2 (BIAcore).

Preparation of Antibodies—Corresponding to the 14 amino acids of the N terminus of human PDZK1, rabbit anti-PDZK1 polyclonal antibody raised against the keyhole limpet hemocyanin-conjugated synthesized peptides, MTSTFNPREC (amino acids 1–10 of the human PDZK1 amino acid sequence), was generated.

Tissue Distribution—Human Multiple Tissue cDNA Panels I and II were purchased from Clontech. Each sample (1.5 μl) was amplified in 50 μl of the PCR mix consisting of 2.5 units of *Taq* Polymerase (Promega), 1× reaction buffer, 1.5 mM $MgCl_2$, and 200 μM dNTP under the following conditions: 35 cycles of 30 s at 95 °C, 30 s at 60 °C, and 1 min at 72 °C for URAT1 and PDZK1; only 25 cycles were performed for β-actin. The PCR products (5 μl) were resolved on a 2% agarose gel. The primers used for PCR amplification are as follows: 5′-CTG GCA ACG GAC TGG AGA TTA-3′ (forward primer for hURAT1), 5′-TGT AGT

AGC GCA CGG GTT GG-3′ (reverse primer for hURAT1), 5′-GAG GAG AAC TTG GAG GTG TT-3′ (forward primer for hPDZK1), 5′-TTT GTA GGC TGG TGA TGA CT-3′ (reverse primer for hPDZK1), 5′-GAG GAG AAC TTG GAG GTG TT-3′ (forward primer for human β-actin), and 5′-TTT GTA GGC TGG TGA TGA CT-3′ (reverse primer for human β-actin).

Immunohistochemical Analysis—The antibodies against human URAT1 used in this study have been shown to be specific for its synthetic peptide, as previously described (4). We used human single-tissue slides (Biochain) for light microscopic immunohistochemical analysis using the streptavidin-biotin-horseradish peroxidase complex technique (LSAB kit; DAKO, Carpentaria, CA). Sections were deparaffinized, rehydrated, and incubated with 3% H_2O_2 for 10 min to abrogate endogenous peroxidase activity. After rinsing in 0.05 M Tris-buffered saline containing 0.1% Tween 20 (TBST), the sections were treated with 10 μg/ml primary rabbit polyclonal antibodies against hURAT1 and hPDZK1 (4 °C overnight). Then, the sections were incubated with the secondary antibody, biotinylated goat polyclonal antibody against rabbit immunoglobulin (DAKO), diluted 1:400 for 30 min with horseradish peroxidase-labeled streptavidin. This step was followed by incubation with diaminobenzidine and hydrogen peroxide. The sections were counterstained with hematoxylin and examined by light microscopy.

Cell Culture and Transfection—Human embryonic kidney 293 (HEK293) cells were maintained in Dulbecco's modified Eagle's medium (DMEM) supplemented with 10% fetal bovine serum, 1 mM sodium pyruvate, 100 units/ml penicillin, and 100 mg/ml streptomycin (Invitrogen) at 37 °C and 5% CO_2. Transient transfection with LipofectAMINE 2000 (Invitrogen) was performed according to the manufacturer's instructions. After transfection, the cells were grown 36–48 h before the experiments. For the establishment of URAT1-expressing cells, stable transfectants were selected for 2 weeks by adding 0.5 mg/ml G418 to the medium.

Immunoprecipitation and Immunoblotting—Twenty-four hours after cotransfection, HEK293 cells in 100-mm plates were lysed with a buffer containing 20 mM Tris (pH 7.4), 250 mM NaCl, 1% Triton X-100, 5 mM EDTA, 0.25% deoxycholate, and protease inhibitor mixture (PIC, Sigma). Lysates were centrifuged at 15,000 rpm for 5 min, and the supernatant was collected. 1 μl of the anti-GFP antibody (Full-Length A.v. Polyclonal Antibody, Clontech) was added to the supernatant, and the mixture was incubated overnight at 4 °C with continuous gentle shaking. For the coimmunoprecipitation of endogenous URAT1 and PDZK1, we used human kidney membrane fractions (Biochain) and added anti-PDZK1 antibody or control IgG to this solution. Then URAT1 and associated proteins were immunoprecipitated using the Seize Classic (A) Immunoprecipitation kit (Pierce), and protein complexes were eluted according to the manufacturer's instructions. The elution samples were resuspended in SDS sample buffer and heated for 5 min at 100 °C, and proteins were resolved on 10% SDS-PAGE gels. The resolved proteins were then electrophoretically transferred to polyvinylidene difluoride membranes. The affinity-purified rabbit PDZK1 antibody and horseradish peroxidase-coupled goat anti-rabbit IgG (Amersham Biosciences) were used for immunoblotting. Immunoblotting was developed with enhanced chemiluminescence reagents (ECL Plus, Amersham Biosciences).

Cell Surface Biotinylation—Surface biotinylation of URAT1 at the plasma membrane was performed as described Huh *et al.* (18) with some modifications. URAT1 stably expressing HEK293 cells transfected with pcDNA3.1(+)-hPDZK1 or pcDNA3.1(+) vector alone were washed three times with phosphate-buffered saline (PBS), and surface proteins were biotinylated with Sulfo-NHS-SS-Biotin (Pierce, 0.5 mg/ml) in PBS for 30 min at 4 °C. Cells were washed with three times with ice-cold PBS containing 50 mM glycine to remove non-reacted chemicals. Cells were harvested, spun at 14,000 × *g* at 4 °C for 4 min to pellet insoluble material, assessed for protein contents, and adjusted to the same concentration. Cell lysates were then incubated with Ultralink-immobilized NeutrAvidin beads (Pierce) to precipitate biotinylated proteins. The bound proteins were eluted with SDS sample buffer and were subjected to SDS-PAGE and Western blotting followed by ECL (Amersham Biosciences). URAT1 was detected with polyclonal URAT1 antibody (1:5,000) (4). Densitometric analysis was performed using Model DIANA II Imaging System (M&S Instruments Trading Inc., Tokyo, Japan).

Urate Transport Activity Assay—HEK293 cells, plated on 24-well culture plates at a density of 2×10^6 cells/well 24 h prior to transfection, were incubated in LipofectAMINE 2000 as described above. After 36 h, the culture medium was removed, and the cells were incubated in serum- and chloride-free Hanks' balanced salt solution containing the following in mM: 125 sodium gluconate, 4.8 K gluconate, 1.2 KH_2PO_4, 1.2 $MgSO_4$, 1.3 calcium gluconate, 5.6 glucose, and 25 HEPES, pH 7.4, for 10 min. The uptake study was started by adding HBSS containing [^{14}C]urate to the plate. Because the uptake of urate was linear up to 5 min in transiently transfected cells and up to 2 min in stably transfected cells, the initial uptake was assessed as the uptake for 1 min (data not shown). After 1 min, the cells were washed twice in ice-cold Hanks' balanced salt solution then lysed in 0.1 N NaOH for 20 min for scintillation counting.

For determination of the kinetic parameters, the concentrations of urate were varied from 100 to 1000 μM. URAT1-mediated urate uptake was calculated as the difference between the values of uptake into HEK293 cells stably expressing URAT1 and those of HEK293 cells transfected vector alone. Kinetic parameters were obtained using Equation 1,

$$v = \frac{V_{max} \times S}{K_m + S} \quad \text{(Eq. 1)}$$

where v is the uptake rate of the substrate (picomoles/min/mg of protein), S is the substrate concentration in the medium (μM), K_m is the Michaelis-Menten constant (μM), and V_{max} is the maximum uptake rate (picomoles/min/mg of protein). These values were determined with the Eadie-Hofstee equation.

Statistical Analysis—Uptake experiments were conducted three times, and each uptake experiment was performed in triplicate. Values were presented as means ± S.D. Statistical significance was determined by non-paired *t* tests.

RESULTS

Isolation of PDZK1 in Yeast Two-hybrid Genetic Screen—In our search for potential URAT1 binding partners, we used the URAT1 C-terminal tail (URAT1-CT) as bait in a yeast two-hybrid screen of a cDNA library constructed from the human adult kidney. From 1.8×10^7 independent colonies screened, 98 positive clones were obtained. Of these positive clones, 35 yielded an identical sequence encoding some portions of the gene for human PDZK1. PDZK1 is a 519-amino acid protein that contains four PDZ domains (19) (GenBank™ accession number NM_002614). The longest clone, 27A, includes PDZ2, PDZ3, and PDZ4 but lacks N-terminal sequences, including half of PDZ1. We could not detect interaction between the URAT1-CT with any other PDZ proteins known to be expressed near the apical membrane of proximal tubules, including NHERF1 and E3KARP (20–22). For further experiments, we cloned full-length human PDZK1 by long PCR and subcloned it into a prey vector.

The specificity of the interaction between PDZK1 and URAT1-CT was further confirmed by yeast two-hybrid assays. First, we tested the specificity of the interaction between PDZK1 and the C termini of other human OAT proteins. PDZK1 interacted with the C terminus of OAT4 with a different PDZ motif (TSL), but not with those of human OAT1, OAT2, or OAT3 (Fig. 1*A*) (23–25).

The C Terminus of URAT1 Is Necessary for the Interaction with PDZK1—To identify the sites in URAT1 that interact with PDZK1, we made three mutant baits. The first one (URAT1-CT-d3) is a bait that lacks the last three residues of URAT1, which are known to play a crucial role in PDZ domain recognition. The second and third ones (F555A and T553A), the extreme C-terminal phenylalanine (0 position) or threonine (−2 position) of URAT1, have been replaced by alanine, which was expected to abolish or strongly suppress the binding of PDZ proteins (10). These three baits did not interact with PDZK1 (Fig. 1*B*). Thus, binding through the C terminus of URAT1 suggests that the PDZ motif of URAT1 is the site of interaction with PDZK1.

Domain Analysis of PDZK1 Protein-Protein Interaction with URAT1 C Terminus—PDZK1 possesses four PDZ domains that assemble target proteins by binding to a C-terminal motif with a consensus sequence such as (S/T)*X*Ø. To determine the possible interactions of the URAT1 C-terminal region with the